

a point-by-point response to the reviews

Response to referee #1's comments

We replied to 9 main comments and 9 minor comments hereafter.

Main Comment

1-3. this paper is about the testing of the GEMS retrieval algorithm on OMI radiances, and the subsequent comparison with ozonesondes. This is interesting and worthwhile study in the run-up to the launch of GEMS. I see the paper as having two main purposes with respect to GEMS. First, it is an exercise of the retrieval algorithm on real OMI data. The fact that this is successful gives confidence that the retrieval is ready to receive the first GEMS data after launch. However, quantitative verification of the retrieval performance is harder, and the discussion of the GEMS retrieval algorithm performance on OMI radiances against sondes, compared with the OMI-algorithm retrievals against the same sondes should be expanded. The second purpose is to identify those ozonesonde measurements that might be good for GEMS validation, in as much as the work here suggests that they are useful or not for OMI validation. If there is a cross-verification here, it is really about OMI validation between OMI and the radiosondes. The fact that the GEMS algorithm is used to process the OMI radiances does not change this, especially with comparisons that should adequately account for how a priori profile and smoothing error assumptions differ between the GEMS and usual OMI algorithms. As such, the title of the manuscript does not clearly describe what is done in the paper, and I suggest that the authors modify the title to better reflect the above two goals.

- As indicated by this reviewer, the simulated GEMS retrievals are similar to OMI retrievals (PROFOZ), but with different and better implementations. Therefore the cross-verification performed in this paper is actually close to OMI validation than GEMS validation. The smoothing errors between OMI and GEMS have been addressed in Bak et al. (2013), indicating that GEMS will provide the comparable ozone profile information below ~ 22 km and the reduced information up to ~ 40 km. The tropopause-based ozone profile climatology is implemented as a priori ozone information for GEMS. However, the goal of this paper is not to detail the difference between OMI and GEMS ozone profile retrievals, but to evaluate the simulated GEMS tropospheric ozone retrievals using the limited UV information (300-330 nm) and to prepare the good reference dataset for GEMS validation. The quality comparison of simulated GEMS retrievals with OMI retrievals are additionally performed to demonstrate the confidence of the presented GEMS ozone profile algorithm. According to reviewer's suggestion, the title is changed to "Cross-evaluation of GEMS tropospheric ozone retrieval performance using OMI data and the use of ozonesonde dataset over East Asia for validation" to clearly reflect what we did through this work.

37
38
39
40
41
42
43
44
45
46
47
48
49
50
51
52
53
54
55
56
57
58
59
60
61
62
63
64
65
66
67
68
69
70
71
72
73
74
75
76

4. Section 2.1 describes the retrieval algorithm applied to the OMI radiances. A discussion should be included as to how the retrieval algorithm characteristics are expected to change for the GEMS radiances.

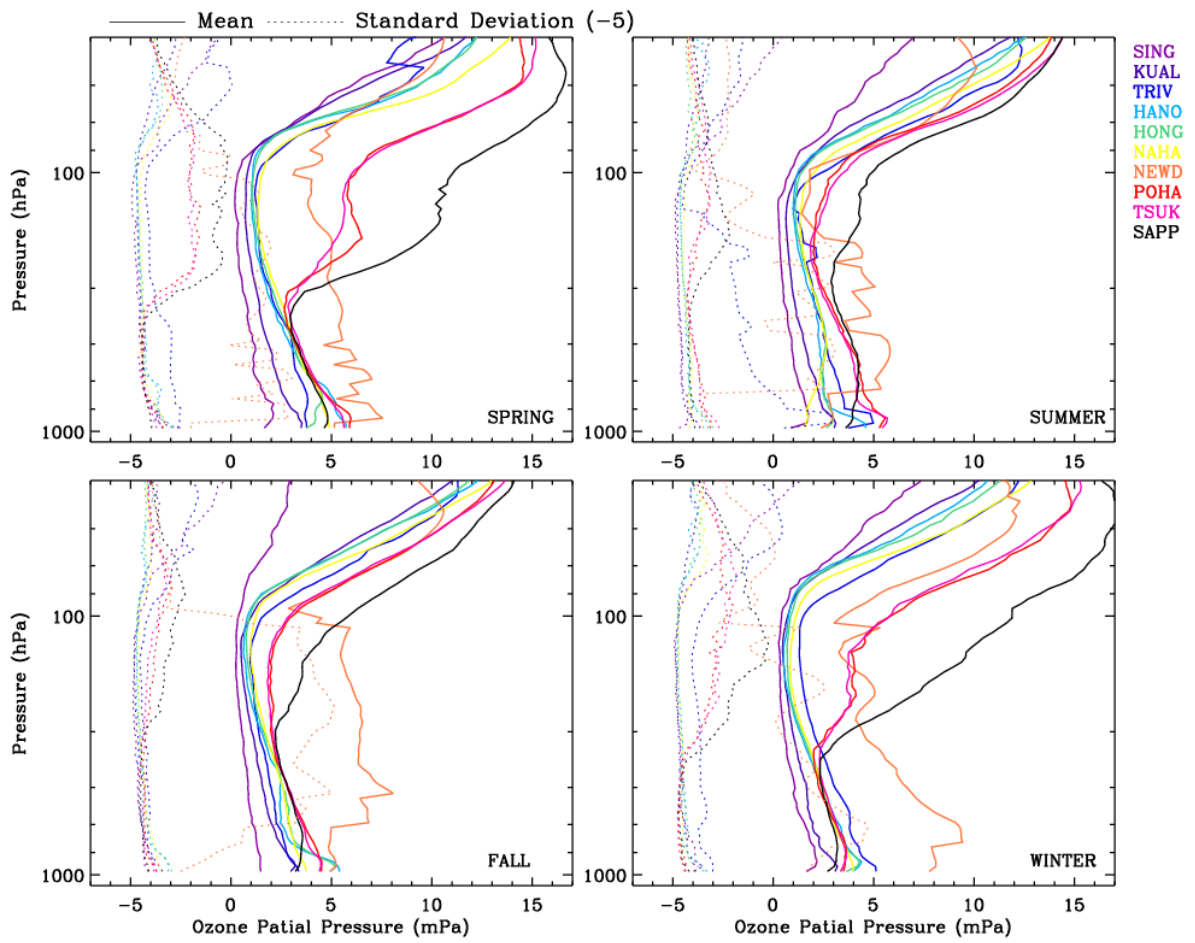
- GEMS is a scanning Uv/Visible spectrometer with a single UV-enhanced CCD for the spectral measurements of 300-500 nm (FWHM: 0.6 nm, spectral sampling: 0.2 nm) with at least comparable radiometric/wavelength accuracy (4% including light source uncertainty/0.01 nm) as OMI. However, GEMS data processing is expected to be different tofrom OMI mainly in two ways: 1) OMI uses a depolarizer to scramble the polarization of light. However, GEMS has polarization sensitivity (required to be less than 2%) and performs polarization correction using an RTM-based look-up table of atmospheric polarization state and pre-flight characterization of polarization instrument polarization sensitivity in the level 0 to 1b data processing. The GEMS polarization correction is less accurate and hence additional fitting process might be required in the level 2 data processing, especially for ozone profiles that have more significant retrieval sensitivityare more sensitive to the polarization error compared to other trace-gases. 2) GEMS has a capability to perform diurnal observations and hence the diurnal meteorological input data are required to account for the temperature dependent Huggins band ozone absorption. Hence, the numerical weather prediction (NWP) model analysis data will be transferred to the GEMS Sscience Ddata Pprocessing Ccenter (SDPC). This part is clarified in the Section 2.1 of the revised manuscript.

5. Section 3.1. The discussion of the differences between satellite/sonde agreements at the different sites is interesting. In addition to the differences between the sonde characteristics and reliabilities, one might expect greater standard deviations at sites that are polluted and/or show greater variability in ozone loadings due to meteorology. Some further discussion would be useful about the chemical-transport environment before eliminating sites from potential GEMS validation based on instrumentation/ experimental method arguments alone. It would also help this reader if the current dense text were broken up into descriptions of the various reasons for good/bad agreement.

- We have added the figure 4 in which the seasonal mean and standard deviations of ozonesonde measurements are presented to see the stability and characteristics of ozonesonde measurements at each site. Instabilities of measurements are observed from New Delhi ozonesondes. High surface ozone concentrations at Trivandrum in summer are believed to be caused by measurement errors because low levels of pollutants have been reported at this site under the geolocation and meteorological effects (Lal et al. 2000). Besides Trivandrum, Naha could be regarded as background sites according to low surface ozone and its precursor concentrations compared to neighboring stations (Fig. 2 and Fig. 4), and previous studies (Oltmans et al., 2004; Liu et al., 2002). In the lower troposphere high ozone concentrations are captured at

77 Pohang, Tsukuba, and Sapporo in the summer due to enhanced photochemical
78 production of ozone in daytime, whereas tropical sites, Naha, Hanoi, and Hong Kong
79 show the ozone enhancement in spring mainly due to biomass burning in Southeast
80 Asia, with low ozone concentrations in summer due to the Asian monsoon and in
81 winter due to the tropical air intrusion (Liu et al., 2002; Ogino et al., 2013). Singapore
82 and Kuala Lumpur are supposed to be severely polluted areas, but ozone pollution is not
83 clearly captured over the seasons. It could be explained by the morning observation
84 time at these two stations. In addition, instabilities of Singapore measurements are
85 noticeable, including abnormally large variability and very low ozone concentration in
86 the stratosphere. The effect of stratospheric intrusions on the ozone profile shape is
87 dominant at mid-latitudes (Pohang, Tsukuba, and Sapporo) during the spring and
88 winter when the ozone pause goes down to 300 hPa, with larger ozone variabilities in
89 the lower stratosphere and upper troposphere, whereas ozone pause is around 100 hPa
90 with much less variability of ozone in other seasons. This discussion has been included
91 in Section 3.

- 92
- 93 ▪ Lal, S., Naja, M., and Subbaraya, B: Seasonal variations in surface ozone and its precursors over an
94 urban site in India, *Atmospheric Environment*, Volume 34, Issue 17, 2000, Pages 2713-2724, 2000.
 - 95 ▪ Liu, H., D. J. Jacob, L. Y. Chan, S. J. Oltmans, I. Bey, R. M. Yantosca, J. M. Harris, B. N. Duncan, and
96 R. V. Martin, Sources of tropospheric ozone along the Asian Pacific Rim: An analysis of ozonesonde
97 observations, *J. Geophys. Res.*, 107(D21), 4573, doi:10.1029/2001JD002005, 2002.
 - 98 ▪ Ogino, S.-Y., M. Fujiwara, M. Shiotani, F. Hasebe, J. Matsumoto, T. H. T. Hoang, and T. T. T. Nguyen
99 (2013), Ozone variations over the northern subtropical region revealed by ozonesonde observations in
100 Hanoi, *J. Geophys. Res. Atmos.*, 118, 3245–3257, doi:10.1002/jgrd.50348.



101
102
103

Fig. 4. Seasonal mean (solid) and standard deviation (dashed) of ozonesonde soundings from 2005 to 2015 at 10 sites. 5 mPa is subtracted to standard deviations to fit in the given x-axis.

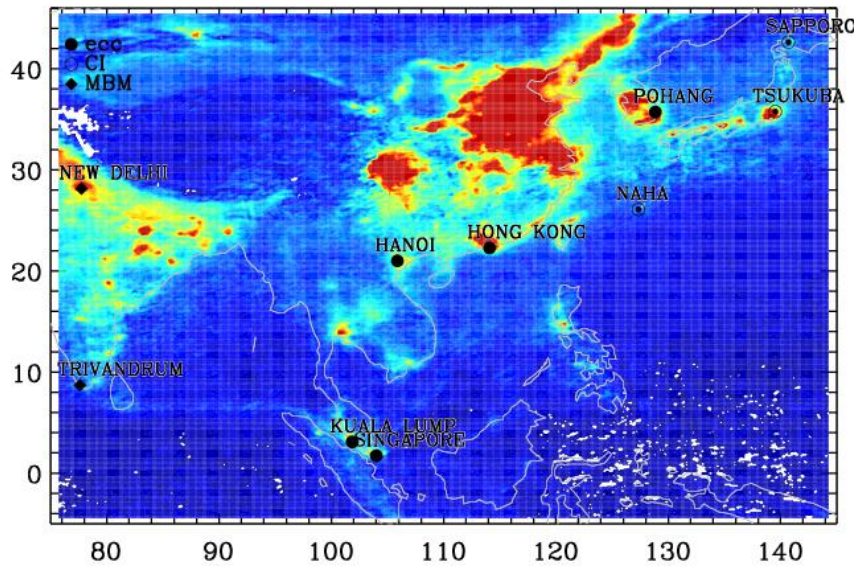
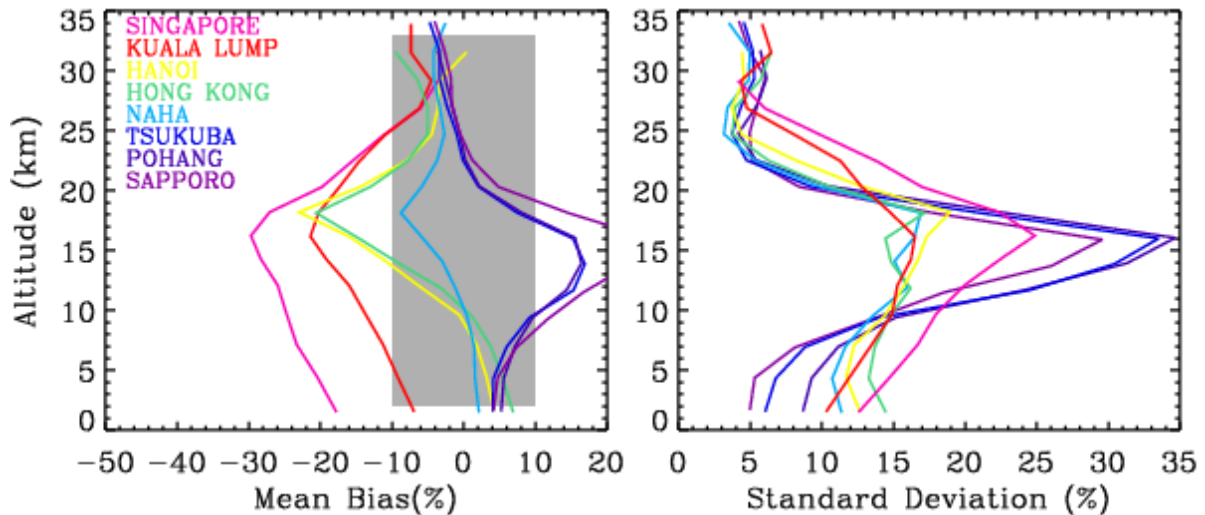


Figure 2. Geographic locations of the ozonesonde stations available since 2005 over the GEMS observation domain. The background map illustrates the OMI NO₂ monthly mean in June 2015.

6. Section 4.2 and Fig. 7. The impact on correlation of smoothing or not smoothing the sonde profiles might be dependent on how close the GEMS retrieval a priori profile is to the sonde “truth”. How do these compare and how do they vary between locations of good and poor comparison? How far does a priori profile go toward explaining the bias?

- To explain this impact, the comparison between GEMS a priori and ozonesondes is presented below, similarly to Fig.6 (in old manuscript, it is Fig. 7 in the revised one). This a priori information is taken from the tropopause-based ozone profile climatology (TB) which adjusts a monthly and zonal mean ozone profile with a daily tropopause height. Bak et al. (2013) demonstrated that TB based a priori better represents the ozone variabilities in the extra-tropical upper troposphere and lower stratosphere, especially during the winter and spring when the atmospheric status is strongly controlled by the dynamics. A priori information is very important to the quality of UV ozone profile retrievals, but the retrieved ozone profiles show much better agreement with ozonesondes than a priori ozone profiles, implying that the independent piece of information are available from these UV measurements. We can see that the biases seen in a priori are significantly reduced for most stations except for the Singapore station. Positive biases around 15 km in the a priori at the three mid-latitude sites still remain in the retrievals but with much smaller magnitude. Negative biases around ~17 km at other lower-latitude sites (except for Singapore) are almost eliminated in the retrievals.



128
129

S1. Same as Fig 6, but for comparison of ozonesondes and a TB-based priori ozone profiles.

131

132 7-8. Section 4.2 should be split into another sub section at Line 354 that starts the discussion
 133 of the evaluation of the GEMS algorithm against the OMI algorithm. This should be presented
 134 as one of the main results sections of this paper: a quantitative evaluation of the GEMS
 135 algorithm against other widely used algorithms based on the same OMI radiances. Given the
 136 previous discussion in the paper of the various limitations of some of the sondes, it might
 137 additionally be useful to directly compare the results of the different retrieval algorithms and
 138 explain differences in results on the basis of different features of the algorithms. This would
 139 help make the case that the GEMS algorithm is performing as expected.

- 140 ▪ In this paper, the ozonesonde measurements available in the GEMS domain are
 141 characterized and validated to better evaluate the performance of the GEMS ozone
 142 profile algorithm. The accuracy and precision of simulated GEMS ozone profiles are
 143 established against the selected true reference. Additionally, the consistent evaluation
 144 is performed for the existing OMI ozone products to check the confidence of the
 145 GEMS retrieval algorithm, demonstrating that the comparable or better performance
 146 of GEMS ozone profile retrievals in the comparison with ozonesonde measurements.
 147 The different validation results between retrieval algorithms were discussed such as
 148 “GEMS algorithm is developed based on the heritages of the SAO ozone profile
 149 algorithm with several modifications. There are two main modifications: a priori ozone
 150 climatology was replaced with a tropopause-based ozone profile climatology to better
 151 represent the ozone variability in the tropopause. Irradiance spectra used to normalize
 152 radiance spectra and characterize instrument line shapes are prepared by taking 31-day
 153 moving average instead of climatological average to take into account for time-
 154 dependent instrument degradations. These modifications reduce somewhat spreads in
 155 deviations of satellite retrievals from sondes, especially in TCO comparison. KNMI
 156 retrievals systematically overestimate the tropospheric ozone by ~ 6 DU (Fig. 9.c),

157 which corresponds to the positive biases of 2-4 % in the integrated total columns of
158 KNMI profiles relative to Brewer observations (Bak et al., 2015). As mentioned in Bak
159 et al. (2015), the systematic biases in ozone retrievals are less visible in SAO-based
160 retrievals (GEMS simulation, OMPROFOZ) as systematic components of measured
161 spectra are taken into account for using an empirical correction called “soft
162 calibration”. The GEMS algorithm is very similar to the SAO algorithm except for the
163 use of TB climatology and the impact of TB on the retrievals was discuss in detail in
164 Bak et al. (2013). Also the comparison of SAO and KNMI algorithms were discussed
165 in detail in Bak et al. (2015). So we think that it is more efficient to place the discussion
166 related to Figures 7-9 in the same section and the direct comparison of GEMS and
167 other OMI product is beyond the scope of this paper.

- 168 ■
- 169 9. The paper requires careful, and extensive, editing for English usage, and cut-paste typos, e.g.
170 line 75, that should have been corrected before manuscript submission.
 - 171 ■ This manuscript is going to be carefully revised though native English co-author
172 before the submission of the revised manuscript.

173 174 **Minor Comments**

- 175 1. Several times “GEMS” measurements are described. The word “simulated” should
176 be added each time to avoid confusion
 - 177 ■ In this revised manuscript, “GEMS measurements” was edited to “ simulated GEMS
178 measurements”
- 179 2. **Line 83:** consistent perhaps, but not homogeneous as the authors point out in the text above.
 - 180 ■ The indicated sentence was revised from “a homogenous, consistent ozonesonde” to
181 “a consistent ozonesonde”.
- 182 4. **Line 105:** Instrument errors certainly, but also instrument design sensitivity.
 - 183 ■ The indicated word, “instrumental errors” was revised to “Instrument errors certainly,
184 but also instrument design sensitivity”
- 185 5. **Line 106:** Common geophysical conditions can reduce sensitivity, not just extreme
 - 186 ■ The associated sentence was edited from “The impact of a priori information on
187 retrievals become important ~ under extreme geophysical conditions to ~ under
188 certain geophysical conditions.
- 189 6. **Line 123:** Information may be limited but is a goal of the GEMS mission. This should be
190 clarified.
 - 191 ■ The GEMS mission was originally planned to develop the spectrometer for measuring
192 the tropospheric pollutants, the spectral coverage of 300-500 nm satisfies to observe
193 the tropospheric ozone as well as the lower/middle stratospheric ozone.
- 194 7. **Line 157:** Any more recent references to new measurement technique and instrumentation?
 - 195 ■ More references (Thompson et al., 2017; Witte et al., 2017; 2018) are added in this
196 sentence.

199
200
201
202
203
204
205
206
207
208
209
210
211
212
213
214

8. Line 200: How do these coincidence criteria for OMI and the sondes affect the results? What is the expected variation within the time and space windows? What is the representativeness uncertainty? How do these results here with the OMI comparison inform on the expected GEMS comparisons with hourly measurements at ~7km resolution?

- As mentioned in Section 2.3, the coincidence criteria between satellite and ozonesonde are: $\pm 1.0^\circ$ in both longitude and latitude and ± 12 hours in time and then the closest pixel is selected. The actual spatiotemporal difference is much smaller than this criteria (57.5 km to 66.6 km, ~3 hours). The close collocation can significantly minimize the effects of spatiotemporal variability on the comparison and therefore GEMS validation accuracy could be enhanced compared to OMI, which is newly included in the summary of this paper (The impact of spatiotemporal variability on the comparison will be much reduced for GEMS due to its higher spatiotemporal resolution (7 km x 8 km @ Seoul, hourly) against OMI (48 km x 13 km @ nadir in UV1, daily).

9. Line 231: Is “troposphere” written where is should be stratosphere?

- The indicated sentence was edited to “much coarser vertical resolution of 10-14 km in the troposphere and 7-11 km in the stratosphere”.

217
218

Response to referee #2’s comments

219 We replied to 4 main comments and 25 minor comments

220 Main Comment

221 **C1.** GEMS ozone profile algorithm is applied to OMI BUV measurements. It should be
222 explained why GEMS radiances has not been simulated instead and what is the impact of using
223 LEO measurements for a GEO instrument.

224 **R1.** The development of the GEMS L2 algorithm has been in progress with OMI measurements
225 because the simulation of the GEMS radiances using the forward model has not been fully
226 implemented. Two main differences in GEMS and LEO (OMI) data processing could be
227 expected: 1) OMI use a depolarizer to scramble the polarization of light. However, GEMS has
228 polarization sensitivity (required to be less than $< 2\%$) and performs polarization correction
229 using RTM-based look-up table of atmospheric polarization state and pre-flight
230 characterization of polarization sensitivity in the level 0 to 1b data processing. The GEMS
231 polarization correction is less accurate and hence additional fitting process might be required
232 in the level 2 data processing, especially for ozone profiles that have more significant retrieval

233 sensitivity to the polarization error compared to other trace-gases. 2) GEMS has a capability to
234 perform diurnal observation and hence the diurnal meteorological input data are required to
235 account for the temperature dependent Huggins band ozone absorption. Hence the numerical
236 weather prediction (NWP) model analysis data will be transferred to the GEMS science data
237 processing center (SDPC). This response has been also included in the revised manuscript, also
238 according to the comment #4 from reviewer 1.

239

240 **C2.** The use of OMI measurements makes the title of the paper confusing as the validation is
241 of OMI using GEMS algorithm, but not of GEMS. This needs to be changed.

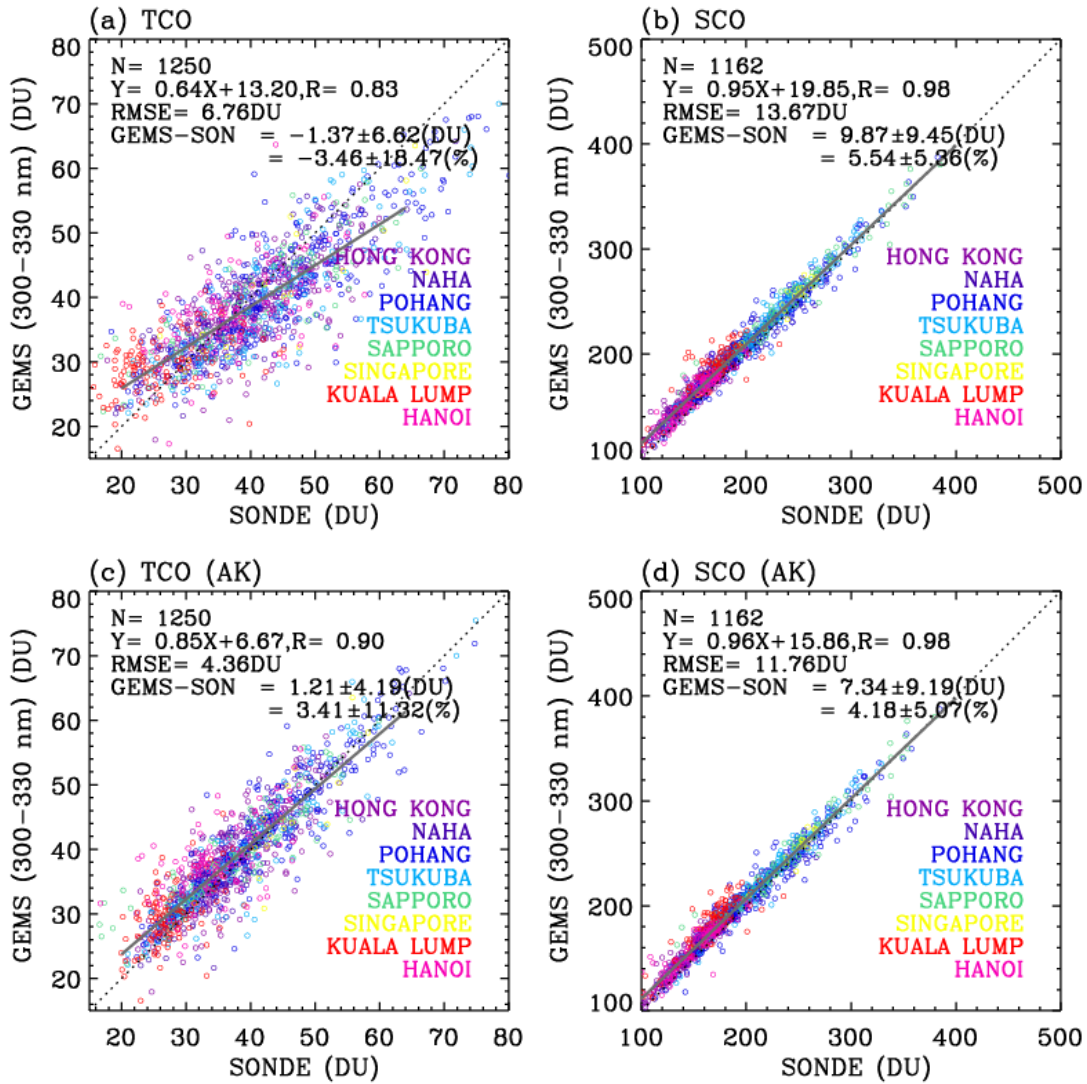
242 **R2.** This reply is also corresponding to comment #1 from reviewer 1, the title of this paper is
243 changed to “Cross-evaluation of GEMS tropospheric ozone retrieval performance using OMI
244 data and the use of ozonesonde dataset over East Asia for validation”.

245

246 **C3.** Simulated GEMS retrievals are used to verify the ozonesonde observations, i.e., to identify
247 the good stations, and in turn, these stations are used to validate the simulated GEMS retrievals.
248 Using this approach it is hard to expect bad results for the simulated GEMS retrievals. The
249 ozonesonde observations should be considered as the truth, and if they need to be validated and
250 screened, this should be done using an independent dataset, but not the same dataset that we
251 intend to validate, in this case the simulated GEMS retrievals.

252 **R3.** Understanding the quality of the reference dataset and then selecting a good reference
253 is a very important process in validating satellite or other in-situ measurements and then in
254 better characterizing the retrieval accuracy and error. Satellite measurements of tropospheric
255 ozone have previously been utilized to disclose problems in ozonesonde observations (e.g., Liu
256 et al., 2006; Huang et al., 2018). We are also using retrievals here to identify ozonesonde
257 measurements with significant errors. However, the station-to-station based quality control has
258 not been typically applied in previous validation works. The figure below demonstrates how
259 much the accuracy of the simulated GEMS retrievals from OMI measurements is
260 underestimated if the station-to-station based quality control is not applied. We also apply the
261 parallel validation for two independent OMI ozone profile products, OMPROFOZ and
262 OMO3PR, respectively, demonstrating that our ozone retrievals are in comparable or better
263 agreement with ozonesondes. As we mentioned in R1 to C1, the simulation of the GEMS

264 radiances using the forward model has not been fully implemented.
 265



266

267 **S1. Same as Figure 8, but for including all ECC measurements.**

268

269

270 **C4.** According to the results shown, the time frame established of ± 12 hours seems too large
 271 for the evaluation of tropospheric ozone, especially for mid-latitudes location where a stronger
 272 daily cycle can be found.

273 **R4.** Based on the previous papers, the collocation of satellite pixel to ozonesonde stations have
 274 been performed within 6 to 24 hours. As clarified in Sect. 2.3 such as “The coincidence criteria

275 between satellite and ozonesonde are: $\pm 1.0^\circ$ in both longitude and latitude and ± 12 hours in
276 time and then the closest pixel is selected. The Aura satellite carrying OMI crosses the equator
277 always at $\sim 1:45$ pm LT and thereby OMI measurements are closely collocated within 3 hours
278 to ozonesonde soundings measured in afternoon (1-3 pm LS),” OMI measurements are closely
279 collocated within 3 hours to ozonesonde soundings measured in afternoon (1-3 pm) from
280 Japanese stations, Pohang, Hong Kong, Hanoi, and Trivandrum. In this paper, the time
281 collocation criterion is set to be 12 hours to include other stations existing over the GEMS
282 domain.

283

284 **Minor comments**

285 **C1.** Line 50: Satellite name should be Sentinel-4

286 **R1.** This name has been corrected to “Sentinel-4”

287

288 **C2.** Line 75: “: : have yet to be not been ...” please correct this

289 **R2.** It has been corrected to “has not been”.

290

291 **C3.** Line 178: Among ECC stations

292 **R3.** It has been corrected to “Among ECC stations”.

293

294 **C4.** Line 183: “Kula lump”, please correct. Also all along the paper, the name of this station is
295 written in different ways (Kuala lump, Kuala Lumpur). Please homogenize the station names
296 in the text, figures and tables.

297 **R4.** We carefully checked what this reviewer indicated. This station name has been corrected
298 to “Kuala Lumpur” across the manuscript.

299

300 **C5.** Line 221: biased -> bias

301 **R5.** It has been corrected to “bias”.

302

303 **C6.** Line 225: Please specify the units

304 **R6.** RMS does not have the unit and thereby “RMS (i.e., root mean square of fitting residuals
305 relative to measurement errors) less than 3” has been kept in the revised manuscript.

306
307
308
309
310
311
312
313
314
315
316
317
318
319
320
321
322
323
324
325
326
327
328
329
330
331
332
333
334
335
336
337

C7. Line 231: troposphere -> stratosphere

R7. It has been corrected to “stratosphere”.

C8. Line 234: Should be photons?

R8. It has been revised to “photons”.

C9. Line 242: x_a should be placed after (1-A)

R9. Eq. 3 has been revised to “ $\hat{x}_{sonde} = A \cdot x_{sonde} + (1 - A)x_a$ ”

C10. Line 282: Please rephrase, maybe “of” -> “with values ranging from”

R10. According to this comment, “satellite retrievals show the distinct seasonal TOC variations with the amplitude of ~ 35-40 DU” has been edited to “~ seasonal TOC variations with the values ranging from ~35 to ~ 40 DU”

C11. Line 290: “Japanese stations” or “stations from Japan”. Same in Line 296.

R11. It has been revised to “stations from Japan”

C12. Line 314: Please unify or explain the differences between LT, LS and LST across the paper

R12. There is no difference. It has been unified to “LT (Local time)”

C13. Line 322: “oznesonde” -> “ozonesonde”

R13. This word has been corrected.

C14. Line 324: Please list stations after “mid-latitude” and refer to Figure justifying this and the following statements.

R14. It has been clarified such as “mid-latitude (Pohang, Tsukuba, and Sapporo)”

C15. Line 326: “- a few %” please rephrase this

R15. It has been corrected to “a few percent”

338 **C16.** Line 338: 4.2 -> 3.2.

339 **R16.** It has been changed to “3.2”.

340

341 **C17.** Line 358: “... gives the good information ...” please rephrase. SOC has not been defined

342 **R17.** It has been corrected to “gives the good information on Stratospheric Ozone Column

343 (SOC)”

344 “

345 **C18.** Line 367: “espeically” -> “especially”. “TCO” -> TOC.

346 **R18.** The relevant sentence has been corrected to “especially in the TOC comparison”

347

348 **C19.** Line 308: Shouldn’t it be “latitudinally” as it is used in other parts of the manuscript?

349 Same in Line 398 and Line 400 (in this case, why capital L?)

350 **R19.** “latitudinally” was used at lines, 27, 308, 398, and 400, respectively. These have been

351 revised as followings,

352 - At 27, “compared to latitudinally adjacent stations with Carbon Iodine (CI) and

353 Electrochemical Condensation Cell (ECC).” to “Carbon Iodine (CI) and Electrochemical

354 Condensation Cell (ECC) dataset measured in similar latitude regime”

355 - At 308, “latitudinally adjacent station, Hong Kong” to “neighboring station, Hong Kong”

356 - At 398, “latitudinally adjacent Japanese 398 ECC measurements at Tsukuba and Sapporo”

357 to “Japanese ECC measurements at Tsukuba and Sapporo located in mid-latitudes (> 30 °)”

358 - At 400, at Naha and Hong Kong stations located in similar latitude regime.

359

360 **C20.** Line 399: Extra s “is similarly”

361 **R20.** This indicated one (is s similarly) has been corrected (is similarly)

362

363 **C21.** Figure 2: Latitudes and Longitudes are not correct.

364 **R21.** This figure has been revised.

365

366 **C22.** Figure 3: Please explain what is CF(O) and CF(X). Even if no CF is applied to MF sondes,

367 it would be interesting to add them in Figure 3.

368 **R22.** To clarify, the legend in the figure has been revised to “Solid: with CF, Dash: w/o CF”.

369 The corresponding caption has been revised to “Effect of applying a correction factor (CF) to
370 (a) ECC and (b) CI ozonesonde measurements, respectively on comparisons with simulated
371 GEMS ozone profile retrievals. Solid and Dashed lines represent the comparisons with and
372 without applying a CF, respectively, at each Japanese station.”

373

374 **C23.** Figure 4: Please specify how you differentiate the different type of sondes. Is it using
375 diamonds, full dots and empty dots? Which one is which? Also indicate what is the horizontal
376 axes, eg. “time (years)”

377 **R23.** This figure has been revised to clarify the symbols and the title of x-axis.

378

379 **C24.** Figure 6: I would suggest rewriting the last sentence as follows “The relative difference
380 (in %) is defined as $100 \times (\text{SONDE AK} - \text{GEMS}) / (\text{A priori})$ ”. Why is multiplied by 2?

381 **R24.** This equation has been corrected to “ $100 \times (\text{SONDE AK} - \text{GEMS}) / (\text{A priori})$ ”

382

383 **C25.** Figure 7 and 8: Please replace TCO -> TOC and SCO -> SOC to be consistent with the
384 text.

385 **R25.** This figure has been revised to accept this comment.

386

387 **a list of all relevant changes**

388 1. All figures have been revised for better visibility, with newly included figure 4.

389 **a marked-up manuscript version**

390

391

392 **Cross-eEvaluation of GEMS tropospheric ozone**
393 **retrieval performance using OMI data and the use**

394 **of ozonesonde dataset over East Asia for**
395 **validation**~~Cross-verification of simulated GEMS-~~
396 ~~tropospheric ozone retrievals and ozonesonde-~~
397 ~~measurements-~~
398 **Over Northeast Asia**

399
400
401 **Juseon Bak**^{1,#} (Juseon.bak@cfa.harvard.edu)

402 **Kang-Hyeon Baek**¹ (iambk100@gmail.com) **Jae-Hwan Kim**^{1,*} (jakim@pusan.ac.kr)

403 **Xiong Liu**² (xliu@cfa.harvard.edu), **Jhoon Kim**³ (jkim2@yonsei.ac.kr) **Kelly Chance**²
404 (kchance@cfa.harvard.edu)

405
406 ¹⁾ Atmospheric Science Department, Pusan National University, Busan, Korea

407 ²⁾ Atomic and Molecular Physics Division, Harvard-Smithsonian Center for Astrophysics, Cambridge, [MA](#), USA-

408 ³⁾ Department of Atmospheric Sciences, Yonsei University, Seoul, Korea

409 #Currently at Atomic and Molecular Physics Division, Harvard-Smithsonian Center for Astrophysics, Cambridge, [MA](#), USA-

410 *Corresponding Author

Abstract

The Geostationary Environment Monitoring Spectrometer (GEMS) is scheduled to be launched in 2019 on board the GEO-KOMPSAT (GEOstationary KOREA Multi-Purpose SATellite)-2B, contributing as the Asian partner of the global geostationary constellation of air quality monitoring. To support this air quality satellite mission, we perform ~~the a~~ cross-verification of simulated GEMS ozone profile retrievals from OMI (Ozone Monitoring Instrument) data based on the Optimal Estimation and ozonesonde measurements within the GEMS domain, covering from 5°S (Indonesia) to 45°N (south of the Russian border) and from 75°E to 145°E. The comparison between ozonesonde and GEMS shows a significant dependence on ozonesonde types. Ozonesonde data measured by Modified Brewer-Master (MBM-M) at Trivandrum and New Delhi show inconsistent seasonal variabilities in ~~the~~ tropospheric ozone, compared to ~~latitudinally adjacent stations with~~ Carbon Iodine (CI) and Electrochemical Condensation Cell (ECC) ozonesondes at other equipped stations in a similar latitude regime. CI ozonesonde measurements are negatively biased relative to ECC measurements by 2-4 DU; ~~a b~~ better agreement ~~with GEMS simulations~~ is achieved ~~with when simulated GEMS ozone retrievals are compared to~~ ECC measurements. ECC ozone data at Hanoi, Kuala Lumpur, and Singapore show abnormally worse agreements with simulated GEMS retrievals ~~among than other~~ ECC measurements. Therefore, ECC ozonesonde measurements at Hong Kong, Pohang, Naha, Sapporo, and Tsukuba are finally identified as an optimal reference dataset. The accuracy of simulated GEMS retrievals is estimated to be ~ 5.0 % for both tropospheric and stratospheric column ozone with the precision of 15 % and 5 %, which meets the GEMS ozone requirements.

434 1. Introduction

435

436 The development of ~~the~~ geostationary ultraviolet (UV)/visible (VIS) spectrometers is ~~highlighted~~
437 ~~toward~~ a new paradigm in the field of the space-based air quality monitoring. It builds on the polar-
438 orbiting instrument heritages for the last 40 years, which were initiated with the launch of a series of
439 Total Ozone Mapping Spectrometer (TOMS) instruments ~~since starting in~~ 1978 (Bhartia et al., 1996)
440 and consolidated by ~~the~~ Global Ozone Monitoring Experiment (GOME) (ESA, 1995), ~~the~~ SCanning
441 Imaging Absorption spectroMeter for Atmospheric CHartographY (SCIAMACHY) (Bovensmann et
442 al., 1999), ~~the~~

443 Ozone Monitoring Instrument (OMI) (Levelt et al, 2006), GOME-2 (EUMETSAT, 2006), ~~the~~
444 Ozone Mapping ~~and~~ Profiler Suite (OMPS) (Flynn et al., 2014), and ~~the~~ TROPOspheric Monitoring
445 Instrument (TROPOMI) (Veefkind et al., 2012). Three geostationary air quality monitoring missions,
446 including the Geostationary Environmental Monitoring Spectrometer (GEMS) (Bak et al., 2013a) over
447 East Asia, Tropospheric Emissions: Monitoring of ~~P~~ollution (TEMPO) (Chance et al, 2013; Zoogman
448 et al., 2017) over North America, and Sentinel-4 (Ingmann et al., 2012) over Europe, are in progress
449 to launch ~~their instruments~~ in the 2019-2022 time frame, ~~which will to~~ provide unprecedented hourly
450 measurements of aerosols and chemical pollutants at sub-urban scale spatial resolution (~ 10-50 km²).
451 These missions will constitute the global geostationary constellation of air quality monitoring.

452 GEMS will be launched in late 2019— ~~or early 2020~~ on board the GeoKOMPSAT-2B
453 (Geostationary Korea Multi-Purpose Satellite) to measure O₃, NO₂, SO₂, H₂CO, CHOCHO, and
454 aerosols in East Asia (Bak et al., 2013a). Tropospheric ozone is a key species to be monitored due to its
455 critical role in controlling ~~the~~ air-quality as a primary component of photochemical smog, ~~the-its~~ self-
456 cleansing capacity as a precursor of the hydroxyl radical, and in controlling the Earth's radiative
457 balance as a greenhouse gas.

458 To support the development of the GEMS ozone profile algorithm, Bak et al. (2013a) demonstrated
459 that the GEMS spectral coverage of 300-500 nm minimizes the loss in the sensitivity to tropospheric
460 ozone despite the lack of most Hartley ozone absorption wavelengths shorter than 300 nm. They further
461 indicated the acceptable quality of the simulated stratospheric ozone retrievals from 212 hPa to 3 hPa
462 (40 km) through comparisons using Microwave Limb Sounder (MLS) measurements. As a consecutive
463 work, this study evaluates simulated GEMS tropospheric ozone retrievals against ozonesonde
464 observations. GEMS ozone retrievals are simulated using an ~~O~~ptimal ~~E~~stimation (~~OE~~) based fitting
465 algorithm ~~from with~~ OMI radiances ~~with using the fitting window of in the spectral range~~ 300-330 nm
466 in the same way as Bak et al. (2013a). The validation effort is essential to ensuring the quality of GEMS

467 ozone profile retrievals and to verifying the newly implemented ozone profile retrieval scheme. In-situ
468 ozonesonde soundings have been considered to be the best reference, but should be carefully used due
469 to ~~its~~ the spatial and temporal irregularities in instrument types, manufacturers, operating procedures,
470 and correction strategies (Deshler et al., 2017). Compared to TEMPO and Sentinel-4, ~~validating the~~
471 ~~GEMS validation activity~~ ~~GEMS ozone retrievals~~ is expected to be more challenging ~~for the ozone~~
472 ~~profile product~~ because of the much sparser distribution of stations and more irregular characteristics
473 of ~~the~~ ozonesonde ~~dataset~~ ~~measurements~~ over the GEMS domain. Continuous balloon-borne
474 observations of ozone are only available ~~from at the~~ Pohang (129.23°E, 36.02°N) site in South Korea,
475 but this site ~~has~~ ~~ve~~ ~~yet to be~~ not been thoroughly validated. Therefore the quality assessment of ~~the~~ ~~its~~
476 ozonesonde data is required before we use this data for GEMS validation ~~activity~~. Compared to
477 ozonesondes, satellite ozone data are less accurate ~~and have much coarser vertical resolution~~, but more
478 homogenous due to ~~its~~ single data processing for the ~~entire~~ measurements from a single instrument.
479 Therefore, abnormal deviations in satellite-ozonesonde differences from neighboring stations might
480 indicate problems at individual stations (Fioletov et al. 2008). For example, Bak et al. (2015) identified
481 27 homogenous stations among 35 global Brewer stations available from the World Ozone and
482 Ultraviolet Radiation Data Centre (WOUDC) network through comparisons with coincident OMI total
483 ozone data. This study adopts ~~this~~ approach to select a ~~homogenous~~, consistent ozonesonde dataset
484 among 10 stations available over the GEMS domain based on ~~the~~ comparisons of the tropospheric ozone
485 columns (TOC) between ~~simulated~~ GEMS retrievals and ozonesonde measurements, that is, simulated
486 GEMS ~~retrievals using OMI data~~ ~~retrievals ones are are is~~ used to verify the ozonesonde observations.
487 The simulated GEMS retrievals are ultimately evaluated against the ozonesonde dataset identified as a
488 true reference to demonstrate the reliability of our future GEMS ozone product. The simulated GEMS
489 retrievals and ozonesonde dataset are described in Sect. 2.1 and 2.2 with the comparison methodology
490 in Sect. 2.3. Our results are discussed in Sect. 3 and summarized in Sect. 4.

491

492 **2. Data and Methodology**

493

494 **2.1 Ozone Profile Retrievals**

495

496 The development of the GEMS ozone profile algorithm builds on ~~the~~ heritages of the Smithsonian
497 Astrophysical Observatory (SAO) ozone profile algorithm which was originally developed for GOME
498 (Liu et al., 2005), continuously adapted for its successors ~~such as including~~ OMI (Liu et al., 2010a),
499 GOME-2 (Cai et al., 2012), and OMPS (Bak et al., 2017). In addition, the SAO algorithm will be

500 implemented to retrieve TEMPO ozone profiles (Chance et al., 2013; Zoogman et al., 2017). In this
 501 algorithm, the well-known optimal estimation (OE) based iterative inversion is applied to estimate the
 502 best ozone concentrations from simultaneously minimizing between measured and simulated
 503 backscattered UV measurements constrained by the measurement covariance matrix, and between
 504 retrieved values and its climatological a priori values constrained by an a priori covariance matrix
 505 (Rodgers, 2000). The impact of a priori information on retrievals becomes important when measurement
 506 information is reduced due to instrumental errors, certainly, but also instrument design sensitivity (e.g.
 507 stray light, dark current, and read-out smear), and ~~or~~ physically insufficient sensitivities under extreme
 508 certain geophysical conditions (e.g. the reduced penetration of incoming UV radiation into the lower
 509 troposphere at high solar zenith angles or, blocked photon penetration below thick clouds). The
 510 described OE-fitting solution \hat{X}_{i+1} can be written, together with cost function χ^2 :

$$\hat{X}_{i+1} = \hat{X}_i + (K_i^T S_y^{-1} K_i + S_a^{-1})^{-1} \{K_i^T S_y^{-1} [Y - R(\hat{X}_i)] - S_a^{-1} (\hat{X}_i - X_a)\} \quad (1)$$

$$\chi^2 = \left\| S_y^{-\frac{1}{2}} K_i (\hat{X}_{i+1} - \hat{X}_i) - [Y - R(\hat{X}_i)] \right\|_2^2 + \left\| S_a^{-\frac{1}{2}} (\hat{X}_{i+1} - X_a) \right\|_2^2 \quad (2)$$

514
 515
 516 Where \hat{X}_{i+1} and \hat{X}_i are current and previous state vectors with a priori vector, X_a and its
 517 covariance error matrix, S_a . Y and $R(X)$ are measured and simulated radiance vectors, with
 518 measurement error covariance matrix, S_y . K is the weighting function matrix ($\frac{dR(x)}{dx}$), describing the
 519 sensitivity of the forward model to small perturbations of the state vector.

520 The ozone fitting window was determined toward maximize the retrieval sensitivity to ozone
 521 and minimize that it to measurement error: 289–307 nm and 326–339 nm for GOME, 270–309 nm
 522 and 312–330 nm for OMI, 289–307 nm and 325–340 nm for GOME-2, and 302.5–340 nm for OMPS.
 523 For OMI, GOME and GOME-2, partial ozone columns are typically retrieved in 24 layers from the
 524 surface to ~ 60 km. However, GEMS (300–500 nm) and OMPS (300–380 nm) do not cover much of the
 525 Hartley ozone absorption wavelengths and hence the reliable profile information of ozone is limited at
 526 least below ~ 40 km (Bak et al., 2013a).

527 Fig. 1 presents is a schematic diagram of the ozone profile algorithm. With the input of satellite
 528 measurements, the slit function is parameterized through cross-correlation between satellite irradiance
 529 and a high-resolution solar reference spectrum to be used for wavelength calibration and for high -
 530 resolution cross section convolution (Sun et al., 2017; Bak et al., 2017); a normalized Gaussian

531 distribution is assumed to derive analytic slit functions for OMI. To remove the systematic errors
532 between measured and calculated radiances, “soft-calibration” is applied to measured radiances and
533 then the logarithms of sun-normalized radiances ~~is-are~~ calculated as ~~a-~~measurement vectors (Liu et al.,
534 2010a; Cai et al., 2012; Bak et al., 2017). ~~A-mM~~Measurement covariance matrices ~~is-are~~ constructed
535 as ~~a-~~diagonal matrices ~~with each-~~components taken from the square of the measurement errors as
536 measurement errors are assumed to be uncorrelated ~~between-among~~ wavelengths;-. In the OMI
537 algorithm, for OMI the noise floor noise of 0.4 % (UV1) and 0.2 % (UV2) is used because OMI
538 measurement errors underestimate other kinds of random noise errors caused by stray light, dark current,
539 geophysical pseudo-random noise errors due to sub-pixel variability, ~~and-~~motion when taking a
540 measurement, forward model parameter error (random part), and other unknown errors into account
541 (Huang et al., 2017). GEMS is expected to have similar retrieval sensitivity to tropospheric ozone,
542 and have at least comparable radiometric/wavelength accuracy (4% including light source
543 uncertainty/0.01 nm) as OMI. A priori ozone information is taken from the tropopause-based (TB)
544 ozone profile climatology; which was developed for improving ozone profile retrievals in the upper
545 troposphere and lower stratosphere (Bak et al., 2013b). The Vector Lnearized Discrete Ordinate
546 Radiative Transfer (VLIDORT) model (Spurr, 2006; 2008) is ~~run-used~~ to calculate ~~the-~~normalized
547 radiances and weighting function matrices ~~for the atmosphere,~~ with Rayleigh scattering and trace-gas
548 absorption and with Lambertian reflection for both surface and cloud (Liu et al., 2010a). The ozone
549 algorithm iteratively estimates the best ozone profiles within the retrieval converges (typically 2-3
550 iterations), together with other geophysical and calibration parameters (e.g., cloud fraction, albedo, BrO,
551 wavelength shifts, Ring parameter, mean fitting scaling parameter) for a better fitting accuracy even
552 though some of the additional fitting parameters can reduce the degrees of freedom for signal of ozone.
553 We should note here that GEMS data processing is expected to be different ~~to~~from OMI mainly in two
554 ways: 1) OMI uses a depolarizer to scramble the polarization of light. However, GEMS has polarization
555 sensitivity (required to be less than 2%) and performs polarization correction using an RTM-based look-
556 up table of atmospheric polarization state and pre-flight characterization of ~~polarization-instrument~~
557 polarization sensitivity in the level 0 to 1b data processing. The GEMS polarization correction is less
558 accurate and hence additional fitting process might be required in the level 2 data processing, especially
559 for ozone profiles that ~~have more significant retrieval sensitivity~~are more sensitive to the polarization
560 error compared to other trace-gases. 2) GEMS has a capability to perform diurnal observations
561 and hence ~~the~~ diurnal meteorological input data are required to account for the temperature dependent
562 Huggins band ozone absorption. Hence, the numerical weather prediction (NWP) model analysis
563 data will be transferred to the GEMS Science Data Processing Center (SDPC).

564

565 2.2 Ozonesonde measurements

566

567 Ozonesondes are small, lightweight, and compact balloon-born instruments capable of measuring
568 profiles of ozone, pressure, temperature and humidity from the surface to balloon burst, usually near 35
569 km (4 hPa); ozone measurements are typically reported in ~~the units~~ of partial pressure (mPa) with ~~the~~
570 vertical resolution of ~ 100-150 m (WMO, 2014). Ozone soundings have been taken for more than 50
571 years, since the 1960s. The accuracy of ozonesonde measurements has been reported as 5-10 % with
572 ~~the~~ precision of 3-5%, depending on the sensor type, manufacturer, solution concentrations, and
573 operational procedure (Smit et al., 2007; Thompson et al., 2007; 2017; Witte et al., 2017; 2018). ~~The~~
574 ~~three~~ types of instruments have been carried on balloons, i.e., the [modified Brewer-Master \(MB-M\)](#),
575 [the carbon iodine cell \(CI\)](#), and the electrochemical concentration cell (ECC), ~~the carbon iodine cell~~
576 ~~(CI)~~. Each sounding is disposable and hence weekly launched for ~~the~~ long-term operation.

577 Fig. 2 displays the locations of 10 ozonesonde sites focused on this study within the ~~expected~~
578 GEMS domain ~~bordering~~ from 5°S (Indonesia) to 45°N (south of the Russian border) and from 75°E
579 to 145°E. A summary of each ozonesonde site is ~~presented~~ in Table 1. Most of measurements are
580 collected from the WOUDC network, except that Pohang soundings are provided from ~~the~~ Korea
581 Meteorological Administration (KMA) and Kuala Lumpur and Hanoi measurements are from the
582 Southern Hemisphere Additional OZonesondes (SHADOZ) network. In South Korea, ECC sondes have
583 been launched every Wednesday since 1995 ~~only~~ at Pohang, without significant time gaps. There are
584 three Japanese stations (Naha, Tsukuba, and Sapporo) where the ~~CI-type~~ sensor was used ~~and before~~
585 ~~switching~~ to the ECC-type sensor as of early 2009, and two Indian stations at New Delhi and
586 Trivandrum using the ~~Modified-modified~~ B-M (MB-M) sensor. The rest of stations (Hanoi, Hong Kong,
587 Kuala Lumpur and Singapore) uses only ECC. Most stations employ ~~an~~ ECC ~~ozone~~ sensors, but
588 inhomogeneities in ECC ozonesondes are strongly ~~addressed with respect~~ ~~correlated~~ to ~~the~~ preparation
589 and correction procedures. There are two ECC sensor manufactures: ~~the~~ Science Pump Corporation
590 (Model type: SPC-6A) and ~~the~~ Environmental Science Corporation (Model type: EN-SCI-Z/1Z/2Z).
591 Since 2011 EN-SCI has been taken over by Droplet Measurement Technologies (DMT) Inc. The
592 Standard Sensing Solution has been recommended as SST1.0 (1.0 % KI, full buffer) and SST 0.5 (2.0 %
593 KI, no buffer) for the SPC and EN-SCI sondes, respectively by the ASOPOS (Assessment for Standards
594 on Operation Procedures for Ozone Sondes) (Smit et al., 2012). Among ECC stations, Pohang, Hong
595 Kong, ~~and the~~ Japanese stations have applied the standard sensing solution to all ECC ~~observation~~
596 ~~sensors manufactured by with its one manufacture one company~~. In Singapore, the ozonesonde
597 manufacture was changed in late 2015 from EN-SCI to SPC, while SST 0.5 was switched to SST 1.0

598 as of 2018. Two SHADOZ stations (~~Kuala Lumpur~~Kuala Lumpur, Hanoi) have applied the standard
599 sensing solution just since 2015. Hanoi changed sensing solution 4 times with two different ozonesonde
600 manufactures; ~~Kuala Lumpur~~ Kula Lumpur operated only with SPC 6A-SST 1.0 combination until 2014,
601 but with four different radiosonde manufactures. Therefore these SHADOZ datasets were ~~reprocessed~~
602 homogenized (~~in~~ Witte et al., (2017) through the application of transfer functions between sensors and
603 solution types ~~to be homogenized~~. The post-processing could be applied by data users to some
604 WOUDC datasets given a correction factor, which is the ratio of integrated ozonesonde column
605 (appended with an estimated residual ozone column above burst altitude) and total ozone measurements
606 from co-located ground-based and/or overpassing satellite instruments. The above-burst column ozone
607 is estimated with a constant ozone mixing ratio (CMR) assumption above the burst altitude (~~e.g.,~~
608 ~~Japanese sites,~~)(Morris et al., 2013) or satellite derived stratospheric ozone climatology (~~e.g.,~~ Indian
609 ~~sites,~~)(Rohtash et al., 2016). No post-processing is ~~given to~~ done for Pohang, Hong Kong, and
610 Singapore. Most stations made weekly or bi-weekly regular observations, except for Indian stations
611 with irregular periods of 0-4 per month and for Singapore with monthly observations.

612 In Fig. 3 the seasonal means and standard deviations of ozonesonde measurements are
613 presented to seeshow the stability and characteristics of ozonesonde measurements at each site.
614 Instabilities of measurements are ~~apparently~~ observed from New Delhi ozonesondes. High
615 surface ozone concentrations at Trivandrum in summer ~~is~~are believed to be caused by
616 measurement errors because low levels of ~~the~~ pollutants ~~has~~have been reported at this site under
617 these geolocation and meteorological effects (Lal et al. 2000). Besides Trivandrum, Naha could
618 be regarded as a background sites according to low surface ozone (Fig. 3) and ~~its~~ precursor
619 concentrations (Fig. 2) compared to neighboring stations, and previous studies (Oltmans et al.,
620 2004; Liu et al., 2002). In the lower troposphere, high ozone concentrations are captured at
621 Pohang, Tsukuba, and Sapporo in the summer due to enhanced photochemical production of
622 ozone in daytime, whereas tropical sites, Naha, Hanoi, and Hong Kong show ~~the~~ ozone
623 enhancements in spring, mainly due to ~~the~~ biomass burning in Southeast Asia, with low ozone
624 concentrations in summer due to the Asian monsoon and in winter due to ~~the~~ tropical air
625 intrusion (Liu et al., 2002; Ogino et al., 2013). Singapore and Kuala Lumpur are supposed to
626 be severely polluted areas, but ozone pollution is not clearly captured over the seasons. ~~It~~This
627 ~~could~~might be explained by the morning observation time at these two stations ~~carried on in~~
628 ~~the morning~~. In addition, instabilities of Singapore measurements are noticeable, ~~such~~
629 ~~as~~including abnormally large variability and very low ozone concentration in the stratosphere.

630 The effect of stratospheric intrusions on the ozone profile shape is dominant at the mid-latitudes
631 (Pohang, Tsukuba, and Sapporo) during the spring and winter when the ozone-pause goes down
632 to 300 hPa, with the larger ozone variabilities in the lower stratosphere and upper troposphere,
633 whereas the ozonepause is placed around 100 hPa with much less variabilities of ozone over
634 the with pressure at in other seasons.

636 2.3. Comparison Methodology

637
638 The GEMS ozone profile algorithm is applied to OMI BUUV measurements ~~in for~~ 300-330 nm to
639 simulate GEMS ozone profile retrievals at coincident locations listed in Table 1. The coincidence
640 criteria between satellite and ozonesondes are: $\pm 1.0^\circ$ in both longitude and latitude and ± 12 hours in
641 time, and then the closest pixel is selected. The Aura satellite carrying OMI crosses the equator always
642 at $\sim 1:45$ pm ~~LT~~ Local Time (LT), and thereby thus OMI measurements are ~~closely~~ collocated within 3
643 hours to ozonesonde soundings ~~measured in the~~ afternoon (1-3 pm ~~LS~~). Weekly-based sonde
644 measurements provide 48 ozone profiles at maximum for a year; the number of collocations is on
645 average 40 from 2004 October to 2008, but reduced to ~ 20 recently due to the screened OMI
646 measurements affected by the “row anomaly” which ~~is was~~ initially detected at two rows in 2007, and
647 seriously spread to other rows with time since January 2009 (Schenkeveld et al., 2017). ~~As f~~From July
648 2011 the row anomaly ~~effect slowly~~ extends up to $\sim 50\%$ of all rows. Correspondingly, the average
649 collocation distance increases from 57.5 km to 66.6 km before and after the occurrence of the row
650 anomaly. The impact of spatiotemporal variability on the comparison will be much reduced for GEMS
651 due to its higher spatiotemporal resolution (7 km \times 8 km @ Seoul, hourly) against OMI (48 km \times 13
652 km @ nadir in UV1, daily).

653 To increase the validation accuracy, ~~the~~ data screening is implemented ~~to for~~ both ozonesonde
654 observations and satellite retrievals according to Huang et al (2017). For ozonesonde observations, we
655 screen ozonesondes with balloon-bursting ~~altitudes pressures~~ exceeding 200 hPa, gaps greater than 3
656 km, abnormally high concentration in the troposphere (> 80 DU), and low concentration in the
657 stratosphere (< 100 DU). Among WOUDC sites, the Japanese and Indian datasets include a correction
658 factor which is derived to make a better agreement between integrated ozonesonde columns and
659 correlated reference total ozone measurements as mentioned in Section 2.2; In Fig. 34, Japanese
660 ozonesondes are compared against GEMS simulations when a correction factor is applied or not to each
661 CI and ECC measurements, respectively. Morris et al. (2013) recommended ~~to restricting~~ the
662 application of this correction factor to the stratospheric portion of the CI ozonesonde profiles due to

663 errors in the above-burst column ozone. Our comparison results illustrate that applying the correction
 664 factor reduces the vertical fluctuation of mean bias~~esed~~ in ozone profile differences with insignificant
 665 impact on their standard deviations. Therefore we decide to apply this correction factor to the sonde
 666 profiles if this factor ranges from 0.85 to 1.15. Because of a lack of retrieval sensitivity to ozone below
 667 clouds and lower tropospheric ozone under extreme viewing condition, ~~satellite retrievals~~GEMS
 668 simulations are limited to cloud fraction less than 0.5, SZAs less than 60°, and fitting RMS (i.e., root
 669 mean square of fitting residuals relative to measurement errors) less than 3.

670 Due to the different units of ozone amount between satellites~~s~~ and ozonesondes~~s~~, we convert
 671 ozonesonde-measured partial pressure ozone values (mPa) to partial column ozone (DU) at the 24
 672 retrieval grids heights of the satellite for the altitude range from surface to the balloon-bursting altitudes.
 673 Ozonesonde measurements are obtained at a rate of a few seconds and then typically averaged into
 674 altitude increments of 100 meters, whereas retrieved ozone profiles from nadir BUV satellite
 675 measurements have much coarser vertical resolution of 10-14 km in the troposphere and 7-11 km in the
 676 ~~stratosphere, troposphere~~ based on OMI retrievals. Consequently, satellite observations~~s~~ captures only
 677 the smoothed structures of ozonesonde soundings, especially ~~in~~-near the tropopause, where a sharp
 678 vertical transition of ozone within 1 km is observed, and in the boundary layer due to the insufficient
 679 penetration of photons~~s~~. Satellite retrievals unavoidably have an error compound due to its limited
 680 vertical resolution, ~~which is named~~called “smoothing error” in ~~the~~OE~~-~~based retrievals (Rodgers, 2000).
 681 It could be useful to eliminate the effect of smoothing errors on differences between satellites~~s~~ and sondes~~s~~
 682 to better characterize other error sources in ~~the~~ comparisons~~s~~ (Liu et al., 2010a). For this reason, satellite
 683 data have been compared to ~~smoothed~~ ozonesonde measurements smoothed ~~into~~ the satellite vertical
 684 resolution~~s~~, together with original sonde soundings (Liu et al., 2010b; Bak et al., 2013b; Huang et al.,
 685 2017). The smoothing approach is: following as

$$687 \quad \hat{x}_{sonde} = A \cdot x_{sonde} + \frac{x_a}{\alpha}(1 - A)x_a \quad (3)$$

688 x_{sonde} : High-resolution ozonesonde profile

689 \hat{x}_{sonde} : Convolved ozonesonde profile into satellite vertical resolution

690 A : Satellite averaging kernel

691 x_a : A priori ozone profile

692
 693 In order to define tropospheric columns, both satellite retrievals and ozonesonde measurements
 694 are vertically integrated from the surface to the tropopause taken from daily National Centers for
 695 Environmental Prediction (NCEP) final (FNL) Operational Global analysis data

696 (<http://rda.ucar.edu/datasets/ds083.2/>). To account for the effect of surface height differences on
697 comparison, ozone amounts ~~of~~ from satellite data below the surface heights of ozonesondes ~~is-are~~ added
698 to tropospheric columns of ozonesonde measurements and vice versa.

699

700 3. Results and Discussions

701

702 3.1 Comparison at individual stations

703

704 Witte et al. (2018) recently compared seven SHADOZ station ozonesonde records, including
705 Hanoi and Kuala Lumpur in the GEMS domain, with total ozone and stratospheric ozone profiles
706 measured by space-borne nadir and limb viewing instruments, respectively. In this comparison, the
707 Hanoi station shows comparable or better agreement with the satellite datasets when compared to other
708 sites. Morris et al. (2013) and Rohtash et al. (2016) thoroughly evaluated ozonesonde datasets over
709 Japanese and Indian sites, respectively, but they did not address their measurement accuracy with
710 respect to those at other stations. Validation of GOME TOC by Liu et al. (2006) showed relatively larger
711 biases at Japanese CI stations and validation of OMI TOC by Huang et al. (2017) showed both larger
712 biases and standard deviations at the India MB-M sites. In South Korea, regular ozonesonde
713 measurements are taken only from Pohang, but these measurements have been insufficiently evaluated;
714 only the stratospheric parts of these measurements were quantitatively assessed against satellite solar
715 occultation measurements by Halogen Occultation Experiment (HALOE) from 1995 to 2004 in Hwang
716 et al. (2006), but only 26 pairs were compared despite ~~its~~ the coarse coincident criteria (48 hours in time,
717 $\pm 4.5^\circ$ in latitude, $\pm 9^\circ$ in longitude). Therefore, it is important to perform ~~the~~ quality assessment of
718 ozonesonde measurements to identify ~~the a~~ reliable reference dataset for GEMS ozone profile validation

719 For this purpose, we illustrate tropospheric ozone columns (TOC) as a function of time ~~and for~~
720 individual stations listed in Table 1, measured with three different types of ozonesonde instruments and
721 retrieved with GEMS simulations (Fig. 45), respectively. The goal of this comparison is to identify any
722 abnormal deviation of ozonesonde measurements relative to satellite retrievals, so we exclude the
723 impact of the different vertical resolutions between instruments and satellite retrievals on this
724 comparison by convolving ozonesonde data with satellite averaging kernels. At mid-latitude sites
725 (Pohang, Sapporo, and Tsukuba) both ozonesonde and ~~satellite-simulated~~ retrievals show the distinct
726 seasonal TOC variations with ~~values ranging from the amplitude of~~ values ranging from ~ 35 to ~ 40 DU. Extratropical sites
727 (Naha, Hong Kong, and Hanoi) show less seasonal variations, ~~of~~ 30 to 50 DU, whereas fairly constant
728 concentrations are observed at Kuala Lumpur and Singapore in the tropics. Both ozonesonde
729 observations and ~~satellite-simulated~~ retrievals illustrate similar seasonal variabilities at these locations.

730 At New Delhi and Trivandrum, on the other hand, MB-M ozonesonde measurements abnormally
731 deviate from 10 DU to 50 DU compared to the corresponding satellite retrievals and ~~latitudinally~~
732 ~~neighboring~~ ozonesonde ~~measurements at stations in similar latitudes regimes~~.

733 In Fig. 5-6 time dependent errors in differences of TOC between ozonesonde and ~~satellite-simulated~~
734 ~~GEMS~~ retrievals are evaluated with the corresponding comparison statistics in Table 2. ~~Satellite~~
735 ~~retrievals~~ ~~Simulated retrievals~~ show strong correlation of ~ 0.8 or much larger with ozonesonde
736 measurements at Pohang, Hong Kong, and three ~~stations from Japan~~ ~~Japan stations~~, and with less
737 correlation of ~ 0.5 at other SHADOZ stations in the tropics. However, Indian stations show poor
738 correlation of 0.24. Mean biases and ~~its~~ standard deviations are much smaller at stations where a strong
739 correlation is observed; they are $\sim 1 \text{ DU} \pm \sim 4 \text{ DU}$ at most ECC stations, but deviated to $\sim 4 \text{ DU} \pm \sim$
740 10 DU at MB-M stations. In conclusion, we should exclude ozonesonde observations measured by MB-
741 M to remove irregularities in a reference dataset for validating both GEMS simulated retrievals in this
742 study and GEMS actual retrievals in future study. Moreover, time series of ozonesonde and ~~satellite~~
743 ~~observations~~ ~~simulated retrievals~~ show a significant transition at three ~~Japanese~~ stations as of late 2008
744 and early 2009 when the ozonesonde instruments ~~was-were~~ switched from CI to ECC. This transition
745 could be affected by space-born instrument degradation, but the impact of balloon-born instrument
746 change on them is predominant based on ~~a~~ less time-dependent degradation pattern at ~~latitudinally~~
747 ~~neighboring~~ stations during this period. CI ozonesondes noticeably underestimates atmospheric ozone
748 by 2-3 DU compared to ECC and thereby GEMS TOC biases relative to CI measurements, ~~—are are~~
749 estimated as -2 to -5 DU, but these biases are reduced to $< 1.5 \text{ DU}$ when compared with ECC. Therefore,
750 we decide to exclude these CI ozonesonde observations for evaluating GEMS simulated retrievals.
751 Compared to other ECC stations, Hanoi ~~S~~ station often changed sensing solution concentrations and pH
752 buffers (Table 1), ~~which might -and hence might~~ cause the irregularities due to remaining errors even
753 though transfer functions were applied to ozonesonde measurements to account for errors due to the
754 different sensing solution (Witte et al., 2017). This fact might affect the relatively worse performance
755 compared to ~~latitudinally adjacent a -neighboring~~ station, Hong Kong, where the 1.0 % KI buffered
756 sensing solution (SST 1.0) to ECC/SPC sensors have been consistently applied.

757 Fig. 6-7 compares differences of ozone profiles between ECC ozonesondes and GEMS simulated
758 retrievals at each station. Among ECC ozonesondes, Singapore's ~~ozonesondes~~ are in the worst
759 agreement with ~~satellite retrievals~~ ~~GEMS simulations~~ in both terms of mean biases and standard
760 deviations, which could be explained by the discrepancy ~~of in~~ collocation time. Sonde observations at
761 Japan, Pohang, Hong Kong, and Hanoi ~~S~~ stations, where balloons were launched in afternoon ($\sim 12-15$
762 ~~LSTLT~~), are collocated within $\sim 1-2$ hours ~~to of~~ OMI ~~that passes the equator at 1301:45 pm LST and~~

~~then reaches the pole within 25 min~~, whereas the time discrepancy increases to 7 hours at Singapore, where ozonesondes are launched in the early morning. Photochemical ozone concentrations are typically denser in the afternoon than in the morning and hence ozonesonde measurements at Singapore are negatively biased relative to afternoon satellite measurements. For the reason mentioned above, the discrepancy in the observation time could ~~also impact on~~ affect this comparison at ~~Kuala Lumpur~~ ~~Kuala Lumpur~~, where sondes were mostly launched in the late morning, 2-3 hours prior to the OMI passing time and thereby ozonesonde measurements tend to be negatively biased. These indicate that diurnal variations of ~~the~~ tropospheric ozone are visible in ~~ozonesonde~~ ~~ozonesonde~~ measurements, emphasizing ~~on the utility of~~ hourly geostationary ozone measurements. The comparison results could be characterized with latitudes. In the mid-latitudes (~~Pohang, Tsukuba, and Sapporo~~), noticeable disagreements are commonly ~~addressed~~ ~~seen in~~ the tropopause region where mean biases/standard deviations are ~10 %/~15% larger than those in the lower troposphere. In the extra-tropics (Hong Kong, Naha), consistent differences of ~~a few~~ ~~%-percent~~ are ~~shown~~ ~~seen~~ over the entire altitude ~~range~~ with standard deviations of 15 % or less below the tropopause (~ 15 km). Hanoi and Kuala Lumpur show significantly larger biases/standard deviations compared to other ECC stations. At Hanoi inconsistencies of solution concentrations and pH buffers might influence ~~on~~ this instability. At Kuala Lumpur the inconsistencies of observation times might be one of the reasons, considering its standard deviations of ~100 min, but mostly less than 30 min at other stations. Therefore, we ~~strictly~~ screen out Singapore, Kuala Lumpur, and Hanoi, together with all M-BM measurements at Indian stations and CI measurements at Japanese stations to improve the validation accuracy of GEMS simulated retrievals in next section. ~~Thus~~ ~~Eventually~~, stations, where the standard procedures for preparing and operating ECC sondes are consistently maintained, are ~~accepted~~ ~~adopted~~ as an optimal reference ~~in for~~ this work.

43.2 Evaluation of GEMS simulated ozone profile retrievals

The GEMS simulated retrievals are assessed against ECC ozonesonde soundings at five stations (Hong Kong, Pohang, Tsukuba, Sapporo, and Naha) identified as a good reference in the previous section. The comparison statistics include mean bias and standard deviation in the absolute/relative differences, correlation coefficients, ~~the~~ linear regression results (slope (a), intercept (b), error); the error of the linear regression is defined as $\frac{1}{n} \sqrt{\sum_i^n (y_{GEMS} - y_{fit})^2}$, $y_{fit} = a \cdot y_{sonde} + b$. In Fig. 78, GEMS simulated retrievals are plotted as ~~a-~~ ~~functions~~ of ozonesondes with and without the vertical resolution smoothing, respectively, for the stratospheric and tropospheric columns. GEMS simulations underestimate the tropospheric ozone by $\sim 2.27 \pm 5.94$ DU and overestimate the stratospheric ozone

796 by $\sim 9.35 \pm 8.07$ DU relative to high-resolution ozonesonde observations. This comparison
797 demonstrates ~~a~~ good correlation coefficients of 0.84 and 0.99 for troposphere and stratosphere,
798 respectively. This agreement is degraded if the rejected ECC sondes (Kuala Lumpur, Hanoi, and
799 Singapore) are included; for example, the slope decreases from 0.68 to 0.64 while the RMSE increases
800 6.35 and 6.76 DU for TOC comparison. Smoothing ozonesonde soundings ~~into~~ to GEMS vertical
801 resolution improves the comparison results, especially for the tropospheric ozone columns; standard
802 deviations are reduced by ~ 5 % with mean biases of less than 1 DU. Similar assessments are performed
803 for OMI standard ozone profiles based on the KNMI OE algorithm (Kroon et al., 2011) hereafter
804 referred to as OMO3PR (KNMI) in Fig. 8-9 and the research product based on the SAO algorithm (Liu
805 et al., 2010) hereafter referred to as OMPROFOZ (SAO) in Fig. 9-10, respectively. It implies that GEMS
806 gives ~~the~~ good information on Stratospheric Ozone Columns (SOCs) comparable to both ~~the~~
807 OMI KNMI and SAO products in spite of ~~excluding insufficient information on most of~~ Hartley ozone
808 ~~band absorption in GEMS~~ in GEMS retrievals. Furthermore, a better agreement of GEMS TOCs with
809 ozonesonde is found than with the others due to different implementation details. As mentioned in 2.1.,
810 the GEMS algorithm is developed based on the heritages of the SAO ozone profile algorithm with
811 several modifications. ~~There are~~ two main modifications are: (1) a priori ozone climatology was
812 replaced with a tropopause-based ozone profile climatology to better represent the ozone variability in
813 the tropopause (2); ~~irradiance spectra used to normalize radiance spectra and characterize instrument~~
814 line shapes are prepared by taking 31-day moving average instead of climatological average to take into
815 account for time-dependent instrument degradations. These modifications reduce somewhat the spreads
816 in deviations of satellite retrievals from sondes, especially in TCO-TOC comparison. KNMI retrievals
817 systematically overestimate the tropospheric ozone by ~ 6 DU (Fig. 9-10.c), which corresponds to the
818 positive biases of 2-4 % in the integrated total columns of KNMI profiles relative to Brewer
819 observations (Bak et al., 2015). As mentioned in Bak et al. (2015), the systematic biases in ozone
820 retrievals are less visible in SAO-based retrievals (simulated GEMS ~~data~~ simulation),
821 as systematic components of measured spectra are taken into account for using an empirical correction
822 called “soft calibration”.

824 4. Summary

825
826 We simulate GEMS ozone profile retrievals from OMI BUV radiances in the range ~~of~~ 300-330 nm
827 using the optimal estimation ~~OE~~-based fitting during the period ~~of~~ 2005-2015 to ensure the performance
828 of the algorithm against coincident ozonesonde observations. There are 10 ozonesonde sites over the
829 GEMS domain from WOUDC, SHADOZ and KMA archives. This paper gives an overview of these

830 ozonesonde observation systems to address inhomogeneities in preparation, operation, and correction
831 procedures which cause discontinuities in individual long-term records or ~~in among adjacent~~ stations.
832 Comparisons between simulated GEMS TOC~~s~~-~~retrievals~~ and ozonesondes illustrate a noticeable
833 dependence on the instrument type. Indian ozonesonde soundings measured by MB-M show severe
834 deviations in seasonal time series of TOC compared to coherent GEMS simulations and ~~neighboring~~
835 ozonesonde observations measured in similar latitude regimes. At Japanese stations, CI ozonesondes
836 underestimate ECC ozonesondes by 2 DU or more and a better agreement with GEMS simulations is
837 found when ECC measurements are compared. Therefore, only ECC ozonesonde measurements are
838 ~~first~~ selected as a reference, in order to ensure a consistent, homogeneous dataset. Furthermore, ECC
839 measurements at Singapore, Kuala Lumpur, and Hanoi are excluded. At Singapore and Kuala Lumpur,
840 observations were performed in the morning and thereby are inconsistent with GEMS retrievals
841 simulated at the OMI overpass time in the afternoon. In addition, the observation time for Kuala Lumpur
842 is inconsistent itself compared to other stations; its standard deviation is ~ 100 min, but for other ECC
843 stations it is less than 30 min. At Hanoi the combinations of sensing solution concentrations and pH
844 buffers changed 4 times during the period of 2005 through 2015. Therefore, GEMS and
845 ~~ozonesonde~~ozonesonde comparisons show larger biases/standard deviations at these stations. Pohang
846 station is unique in South Korea where ECC ozonesondes have been regularly and consistently launched
847 without a gap since 1995; the standard 1% KI full buffered sensing solution has been consistently
848 applied to ozone sensors manufactured by SPC (6A model). Evaluation of Pohang ozonesondes against
849 GEMS simulations demonstrates its high level reliability, which is comparable to ~~latitudinally~~
850 ~~adjacent~~~~neighboring~~ Japanese ECC measurements at Tsukuba and Sapporo. Reasonable agreement with
851 GEMS simulated retrievals is ~~s~~similarly shown at ~~Latitudinally~~-adjacent Naha and Hong Kong stations.
852 Finally, we establish that the comparison statistics of GEMS simulated retrievals and optimal reference
853 dataset is $-2.27 (4.92) \pm 5.94 (14.86)$ DU (%) with $R = 0.84$ for the tropospheric columns and 9.35
854 $(5.09) \pm 8.07 (4.60)$ DU (%) with $R=0.99$ for the stratospheric columns. This estimated accuracy and
855 precision is comparable to OMI products for the stratospheric ozone column and even better for the
856 tropospheric ozone column due to improved algorithm implementations. Our future study aims to
857 achieve this quality level from actual GEMS ozone profile product.

858
859 *Author contributions.* JB and KHB designed the research; JHK and JK provided oversight and
860 guidance; JB conducted the research and wrote the paper; XL and KC contributed to the
861 analysis and writing.

862 *Competing interests.* The authors declare that they have no conflict of interest.

863

864

865

Acknowledgement

866 The ozonesonde data used in this study were obtained through the WOUDC, SHADOZ and KMA
867 archives. We also acknowledge the OMI Science Team for providing their satellite data. Research at
868 the Smithsonian Astrophysical Observatory was funded by NASA and the Smithsonian Institution.
869 Research at Pusan National University was supported by Basic Science Research Program through the
870 National Research Foundation of Korea (NRF) funded by the Ministry of Education
871 (2016R1D1A1B01016565). This work was also supported by the Korea Ministry of Environment
872 (MOE) as the Public Technology Program based on Environmental Policy (2017000160001).

873

874

875

Reference

- 876 Bak, J., Kim, J. H., Liu, X., Chance, K., and Kim, J.: Evaluation of ozone profile and tropospheric ozone retrievals
877 from GEMS and OMI spectra, *Atmos. Meas. Tech.*, 6, 239-249, doi:10.5194/amt-6-239-2013, 2013a.
- 878 Bak, J., Liu, X., Wei, J. C., Pan, L. L., Chance, K., and Kim, J. H.: Improvement of OMI ozone profile retrievals
879 in the upper troposphere and lower stratosphere by the use of a tropopause-based ozone profile climatology,
880 *Atmos. Meas. Tech.*, 6, 2239–2254, doi:10.5194/amt-6-2239-2013, 2013b.
- 881 Bak, J., Liu, X., Kim, J.-H., Haffner, D. P., Chance, K., Yang, K., and Sun, K.: Characterization and correction of
882 OMPS nadir mapper measurements for ozone profile retrievals, *Atmos. Meas. Tech.*, 10, 4373-4388,
883 <https://doi.org/10.5194/amt-10-4373-2017>, 2017.
- 884 Bhartia, P. K., McPeters, R. D., Mateer, C. L., Flynn, L. E., and Wellemeyer, C.: Algorithm for the estimation of
885 vertical ozone profiles from the backscattered ultraviolet technique, *J. Geophys. Res.*, 101, 18793–18806,
886 1996.
- 887 Bovensmann, H., Burrows, J. P., Buchwitz, M., Frerick, J., Noel, S., Rozanov, V. V., Chance, K. V., and Goede,
888 A. P. H.: SCIAMACHY: Mission objectives and measurement modes, *J. Atmos. Sci.*, 56, 127–150,
889 doi:10.1175/1520-0469(1999)056<0127:SMOAMM>2.0.CO;2, 1999.
- 890 Cai, Z., Liu, Y., Liu, X., Chance, K., Nowlan, C. R., Lang, R., Munro, R., and Suleiman, R.: , Characterization
891 and correction of Global Ozone Monitoring Experiment 2 ultraviolet measurements and application to ozone
892 profile retrievals, *J. Geophys. Res.*, 117, D07305, doi: 10.1029/2011JD017096, 2012.
- 893 Chance, K., Liu, X., Suleiman, R. M., Flittner, D. E., Al-Saadi, J., and Janz, S. J.: Tropospheric emissions:
894 monitoring of pollution (TEMPO), *Proc. SPIE 8866, Earth Observing Systems XVIII*, 8866, 88660D-1–
895 88660D-16, doi:10.1117/12.2024479, 2013.
- 896 Deshler, T., Stübi, R., Schmidlin, F. J., Mercer, J. L., Smit, H. G. J., Johnson, B. J., Kivi, R., and Nardi, B.: Methods
897 to homogenize electrochemical concentration cell (ECC) ozonesonde measurements across changes in sensing
898 solution concentration or ozonesonde manufacturer, *Atmos. Meas. Tech.*, 10, 2021-2043,

899 <https://doi.org/10.5194/amt-10-2021-2017>, 2017.

900 European Space Agency: The GOME Users Manual, ESA Publ. SP-1182, Publ. Div., Eur. 488 Space Res. and
901 Technol. Cent., Noordwijk, The Netherlands, 1995.

902 European Organization for the Exploitation of Meteorological Satellites (EUMETSAT): GOME-2 level 1 Product
903 Generation Specification, Rep. EPS.SYS.SPE.990011, Darmstadt, Germany, 2006.

904 Fioletov, V. E., Labow, G., Evans, R., Hare, E. W., Khler, U., McElroy, C. T., Miyagawa, K., Redondas, A.,
905 Savastiouk., V., Shalamyansky, A. M., Staehelin, J., Vanicek, K., and Weber, M.: Performance of the ground-
906 based total ozone network assessed using satellite data, *J. Geophys. Res.*, 113, D14313, doi:
907 10.1029/2008JD009809, 2008.

908 Flynn, L., Long, C., Wu, X., Evans, R., Beck, C. T., Petropavlovskikh, I., McConville, G., Yu, W., Zhang, Z., Niu,
909 J., Beach, E., Hao, Y., Pan, C., Sen, B., Novicki, M., Zhou, S., and Seftor, C. : Performance of the Ozone
910 Mapping and Profiler Suite (OMPS) products, *J. Geophys. Res. Atmos.*, 119, 6181–6195, doi:
911 10.1002/2013JD020467, 2014.

912 Hwang, S.-H., J. Kim, J., and Cho, G.-R., Observation of secondary ozone peaks near the tropopause over the
913 Korean peninsula associated with stratosphere-troposphere exchange, *J. Geophys. Res.*, 112, D16305, doi:
914 10.1029/2006JD007978, 2007.

915 Huang, G., Liu, X., Chance, K., Yang et al. : Validation of 10-year SAO OMI Ozone Profile (PROFOZ) Product
916 Using Ozonesonde Observations, *Atmos. Meas. Tech. Discuss.*, doi: 10.5194/amt-2017-15, 2017.

917 Ingmann, P., Veihelmann, B., Langen, J., Lamarre, D., Stark, H., and Courrèges-Lacoste, G. B.: Requirements for
918 the GMES atmosphere service and ESA's implementation concept: Sentinels-4/-5 and-5p, *Remote Sens.*
919 *Environ.*, 120, 58–69, doi:10.1016/j.rse.2012.01.023, 2012.

920 Kroon, M., de Haan, J. F., Veeffkind, J. P., Froidevaux, L., Wang, R., Kivi, R., and Hakkarainen, J. J.: Validation
921 of operational ozone profiles from the Ozone Monitoring Instrument, *J. Geophys. Res.*, 116, D18305, doi:
922 10.1029/2010JD015100, 2011.

923 [Lal, S., Naja, M., and Subbaraya, B: Seasonal variations in surface ozone and its precursors over an urban site in](#)
924 [India, Atmospheric Environment, Volume 34, Issue 17, 2000, Pages 2713-2724, 2000.](#)

925 Levelt, P. F., van den Oord, G. H. J., Dobber, M. R., Malkki, A., Visser, H., de Vries, J., Stammes, P., Lundell, J.
926 O. V., and Saari, H.: The Ozone Monitoring Instrument, *IEEE Trans. Geosci. Remote Sens.*, 44(5), 1093–1101,
927 doi:10.1109/TGRS.2006.872333, 2006.

928 [Liu, H., D. J. Jacob, L. Y. Chan, S. J. Oltmans, I. Bey, R. M. Yantosca, J. M. Harris, B. N. Duncan, and R. V.](#)
929 [Martin. Sources of tropospheric ozone along the Asian Pacific Rim: An analysis of ozonesonde observations,](#)
930 [J. Geophys. Res., 107\(D21\), 4573, doi:10.1029/2001JD002005, 2002.](#)

931 Liu, X., Chance, K., Sioris, C. E., Spurr, R. J. D., Kurosu, T. P., Martin, R. V., and Newchurch, M. J.: Ozone
932 profile and tropospheric ozone retrievals from Global Ozone Monitoring Experiment: algorithm description
933 and validation, *J. Geophys. Res.*, 110, D20307, doi: 10.1029/2005JD006240, 2005.

934 Liu, X., Chance, K., Sioris, C. E., Kurosu, T. P., and Newchurch, M. J. : Intercomparison of GOME, ozonesonde,
935 and SAGE II measurements of ozone: Demonstration of the need to homogenize available ozonesonde data

- 936 sets, *J. Geophys. Res.*, 111, D14305, doi:10.1029/2005JD006718, 2006.
- 937 Liu, X., Bhartia, P.K, Chance, K, Spurr, R.J.D., and Kurosu, T.P.: Ozone profile retrievals from the ozone
938 monitoring instrument. *Atmos. Chem. Phys.*, 10, 2521–2537, 2010a.
- 939 Liu, X., Bhartia, P. K., Chance, K., Froidevaux, L., Spurr, R. J. D., and Kurosu, T. P.: Validation of Ozone
940 Monitoring Instrument (OMI) ozone profiles and stratospheric ozone columns with Microwave Limb Sounder
941 (MLS) measurements, *Atmos. Chem. Phys.*, 10, 2539–2549, doi:10.5194/acp-10-2539-2010, 2010b.
- 942 Morris, G. A., Labow, G., Akimoto, H., Takigawa, M., Fujiwara, M., Hasebe, F., Hirokawa, J., and Koide, T.: On
943 the use of the correction factor with Japanese ozonesonde data, *Atmos. Chem. Phys.*, 13, 1243-1260,
944 <https://doi.org/10.5194/acp-13-1243-2013>, 2013.
- 945 [Ogino, S.-Y., M. Fujiwara, M. Shiotani, F. Hasebe, J. Matsumoto, T. H. T. Hoang, and T. T. T. Nguyen \(2013\),](#)
946 [Ozone variations over the northern subtropical region revealed by ozonesonde observations in Hanoi, J.](#)
947 [Geophys. Res. Atmos., 118, 3245–3257, doi:10.1002/jgrd.50348.](#)
- Petropavlovskikh, I., Evans, R., McConville, G., Oltmans, S., Quincy, D., Lantz, K., Disterhoft, P., Stanek, M.,
and Flynn, L.: Sensitivity of Dobson and Brewer Umkehr ozone profile retrievals to ozone cross-sections and
stray light effects, *Atmos. Meas. Tech.*, 4, 1841–1853, doi:10.5194/amt-4-1841-2011, 2011.
- Rodgers, C. D.: *Inverse Methods for Atmospheric Sounding: Theory and Practice*, World Scientific Publishing,
Singapore, 2000.
- Rohtash, Mandal, T.K., Peshin, S.K. S. K. Peshin and Sharma1, S. K., Study on Comparison of Indian Ozonesonde
Data with Satellite Data, *MAPAN-Journal of Metrology Society of India* 31: 197.doi:10.1007/s12647-016-
0174-4, 2016.
- Schenkeveld, V. M. E., Jaross, G., Marchenko, S., Haffner, D., Kleipool, Q. L., Rozemeijer, N. C., Veeffkind, J.
P., and Levelt, P. F.: In-flight performance of the Ozone Monitoring Instrument, *Atmos. Meas. Tech.*, 10,
1957-1986, <https://doi.org/10.5194/amt-10-1957-2017>, 2017.
- Smit, H. G. J., Straeter, W., Johnson, B., Oltmans, S., Davies, J., Tarasick, D. W., Hoegger, B., Stubi, R., Schmidlin,
F., Northam, T., Thompson, A., Witte, J., Boyd, I., and Posny, F.: Assessment of the performance of ECC-
ozonesondes under quasi-flight conditions in the 10 environmental simulation chamber: Insights from the
Juelich Ozone Sonde Intercomparison Experiment (JOSIE), *J. Geophys. Res.*, 112, D19306, doi:
10.1029/2006JD007308, 2007.
- Smit,, H. G. J., and the Panel for the Assessment of Standard Operating Procedures for Ozonesondes (ASOPOS) :
Guidelines for homogenization of ozonesonde data, SI2N/O3S-DQA activity as part of “Past changes in the
vertical distribution of ozone assessment”. [Available at [http://www-
das.uwyo.edu/%7Edeshler/NDACC_O3Sondes/O3s_DQA/O3S-DQA-Guidelines%20Homogenization-V2-
19November2012.pdf](http://www-das.uwyo.edu/%7Edeshler/NDACC_O3Sondes/O3s_DQA/O3S-DQA-Guidelines%20Homogenization-V2-19November2012.pdf)], 2012.
- Sun, K., Liu, X., Huang, G., Gonzalez Abad, G, Cai, Z., Chance, K., and Yang, K. : Deriving the slit functions
from OMI solar observations and its implications for ozone-profile retrieval, *Atmos. Meas. Tech.*, 10, 3677-
3695, <https://doi.org/10.5194/amt-10-3677-2017>, 2017.

- Spurr, R. J.: VLIDORT: A linearized pseudo-spherical vector discrete ordinate radiative transfer code for forward model and retrieval studies in multilayer multiple scattering media, *J. Quant. Spectrosc. Ra.*, 102, 316–342, doi:10.1016/j.jqsrt.2006.05.005, 2006.
- Spurr, R. J. D.: Linearized pseudo-spherical scalar and vector discrete ordinate radiative transfer models for use in remote sensing retrieval problems, in: *Light Scattering Reviews*, edited by: Kokhanovsky, A., Springer, New York, 2008.
- Veefkind, J. P., Aben, I., McMullan, K., Förster, H., de Vries, J., Otter, G., Claas, J., Eskes, H. J., de Haan, J. F., Kleipool, Q., van Weele, M., Hasekamp, O., Hoozeveld, R., Landgraf, J., Snel, R., Tol, P., Ingmann, P., Voors, R., Kruizinga, B., Vink, R., Visser, H. and Levelt, P. F.: TROPOMI on the ESA Sentinel-5 Precursor: A GMES mission for global observations of the atmospheric composition for climate, air quality and ozone layer applications, *Remote Sensing of Environment*, 120(0), 70–83, doi:10.1016/j.rse.2011.09.027, 2012.
- Thompson, A. M., Stone, J. B., Witte, J. C., Miller, S. K., Oltmans, S. J., Kucsera, T. L., Ross, K. L., Pickering, K. E., Merrill, J. T., Forbes, G., Tarasick, D. W., Joseph, E., Schmidlin, F. J., McMillan, W.W., Warner, J., Hints, E. J., and Johnson, J. E.: Intercontinental Chemical Transport Experiment Ozone Network Study (IONS) 2004: 2. Tropospheric ozone budgets and variability over northeastern North America, *J. Geophys. Res.*, 112, D12S13, doi:10.1029/2006JD007670, 2007.
- Thompson, A. M., Witte, J. C., Sterling, C., Jordan, A., Johnson, B. J., Oltmans, S. J., Fujiwara, M., Vömel, H., Allaart, M., Pitters, A., Coetzee, J. G. R., Posny, F., Corrales, E., Andres Diaz, J., Félix, C., Komala, N., Lai, N. Maata, M., Mani, F., Zainal, Z., Ogino, S.-Y., Paredes, F., Bezerra Penha, T. L., Raimundo da Silva, F., Sallons-Mitro, S., Selkirk, H. B., Schmidlin, F. J., Stuebi, R., and Thiongo, K.: First reprocessing of Southern Hemisphere Additional Ozonesondes (SHADOZ) Ozone Profiles (1998-2016). 2. Comparisons with satellites and ground-based instruments, *J. Geophys. Res.*, JD027406, <https://doi.org/10.1002/2017JD027406>, 2017.
- WMO: Scientific Assessment of Ozone Depletion: 2014, Global Ozone Research and Monitoring Project-Report No. 55, 416 pp., Geneva, Switzerland, 2014.
- Witte J.C., Thompson A.M., Smit H.G.J., Fujiwara M., Posny F., Coetzee G.J.R., Northam E.T., Johnson B.J., Sterling C.W., Mohamad M., Ogino S.- Y., Jordan A., da Silva F.R.: First reprocessing of Southern Hemisphere Additional 20 Ozonesondes (SHADOZ) profile records (1998–2015): 1. Methodology and evaluation, *J. Geophys. Res. Atmos.*, 122, 6,611-6,636, 2017.
- Witte J.C., Thompson A.M., Smit H.G.J., Vömel H., Posny F., Stübi R.: First reprocessing of Southern Hemisphere Additional Ozonesondes profile records: 3. Uncertainty in ozone profile and total column. *J. Geophys. Res. Atmos.*, 123, 2018.
- Zoogman, P., Liu, X., Suleiman, R. M., Pennington, W. F., Flittner, D. E., Al-Saadi, J. A., Hilton, B. B., Nicks, D. K., Newchurch, M. J., Carr, J. L., Janz, S. J., Andraschko, M. R., Arola, A., Baker, B. D., Canova, B. P., Chan Miller, C., Cohen, R. C., Davis, J. E., Dussault, M. E., Edwards, D. P., Fishman, J., Ghulam, A., González Abad, G., Grutter, M., Herman, J. R., Houck, J., Jacob, D. J., Joiner, J., Kerridge, B. J., Kim, J., Krotkov, N. A., Lamsal, L., Li, C., Lindfors, A., Martin, R. V., McElroy, C. T., McLinden, C., Natraj, V., Neil, D. O., Nowlan, C. R., O'Sullivan, E. J., Palmer, P. I., Pierce, R. B., Pippin, M. R., Saiz-Lopez, A., Spurr, R. J. D., Szykman, J. J., Torres, O., Veefkind, J. P., Veihelmann, B., Wang, H., Wang, J., and Chance, K.:

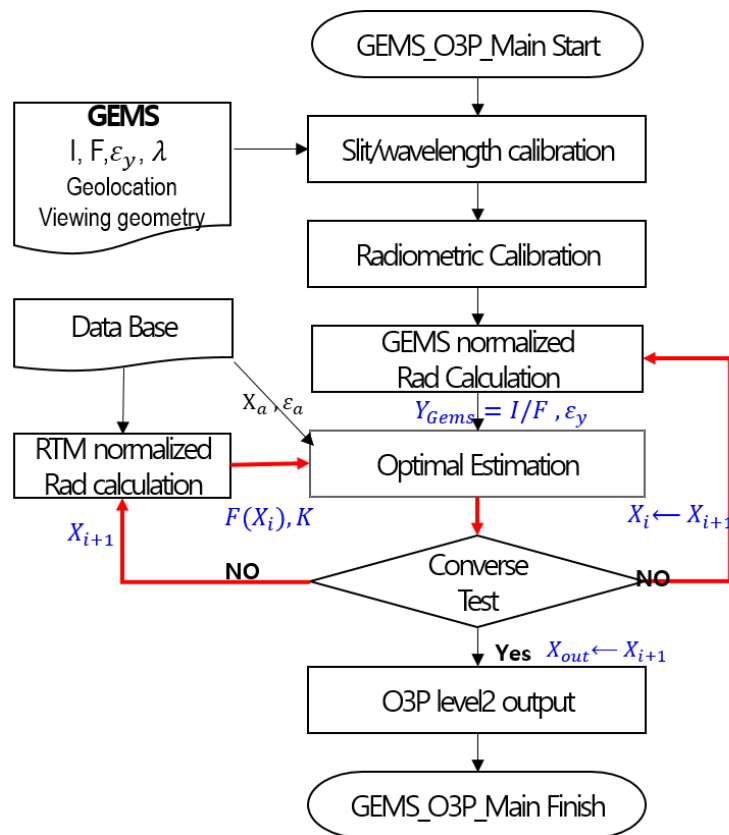


Figure 1. Flow chart of the GEMS ozone profile retrieval algorithm.

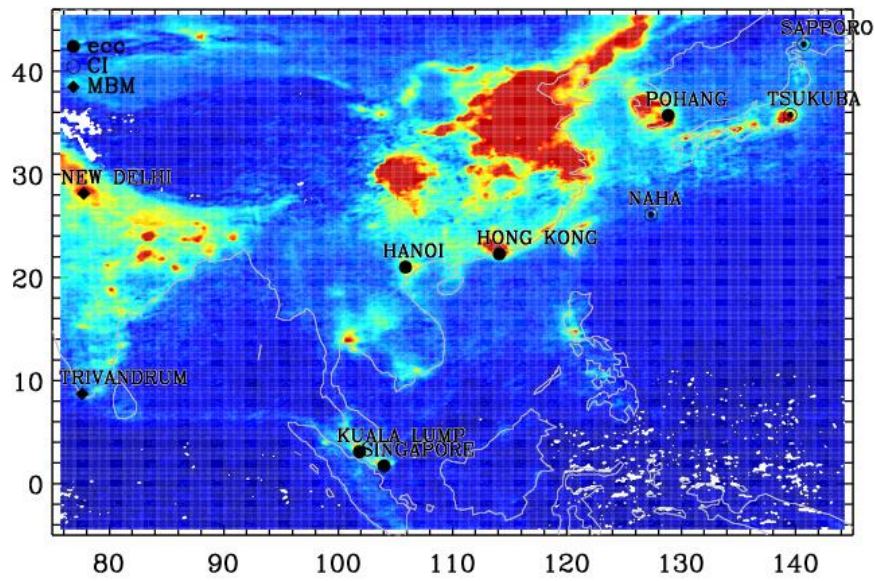


Figure 2. Geographic locations of the ozonesonde stations available since 2005 over the GEMS observation domain. Each symbol represents a different type of sensors; the modified Brewer-Mast (MBM), the carbon iodine cell (CI), and the electrochemical concentration cell (ECC). The background map illustrates the OMI NO₂ monthly mean in June 2015.

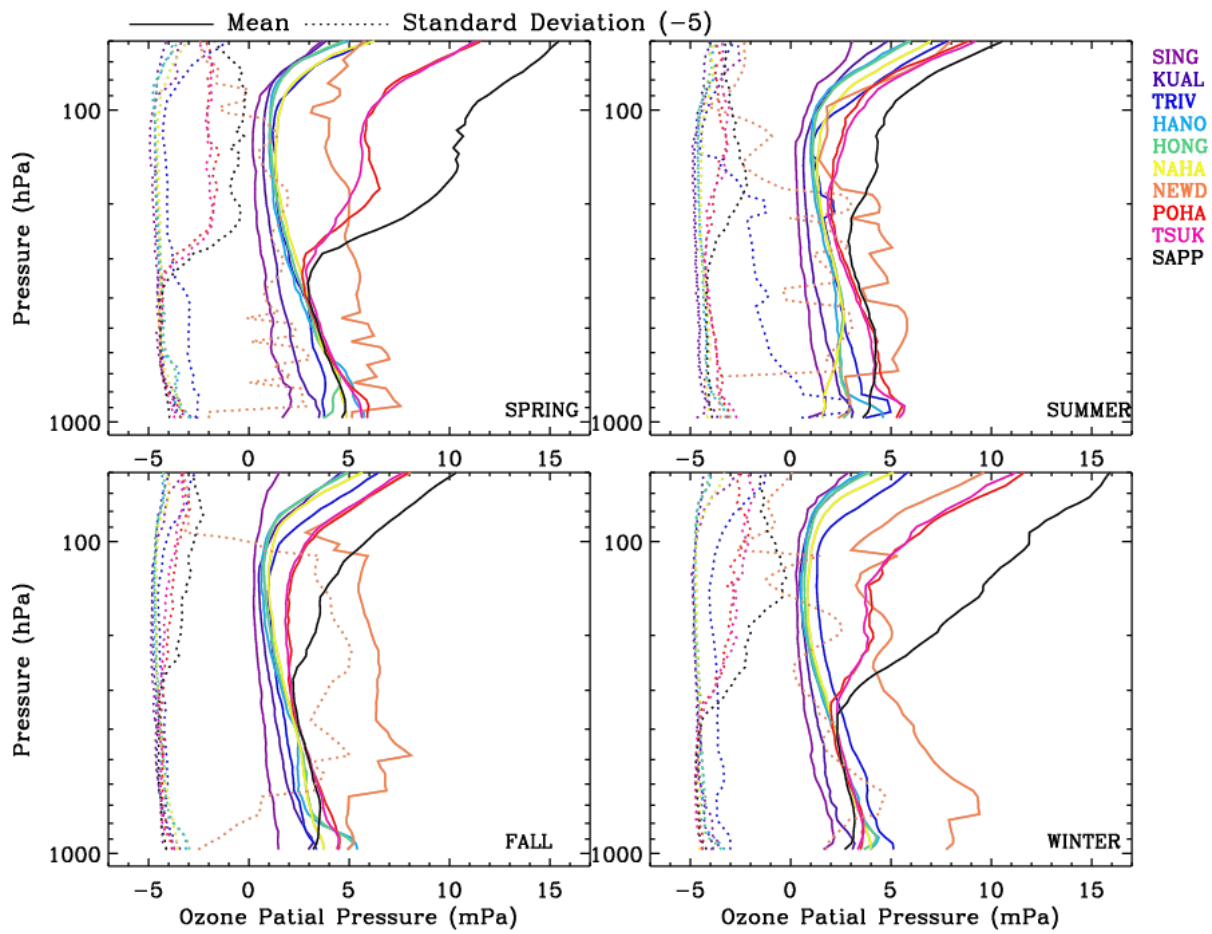


Figure 3. Seasonal mean (solid) and standard deviation (dashed) profiles of ozonesonde soundings from 2005 to 2015 at the 10 sites listed in Table 1. 5 mPa is subtracted from standard deviations to fit in the given x-axis.

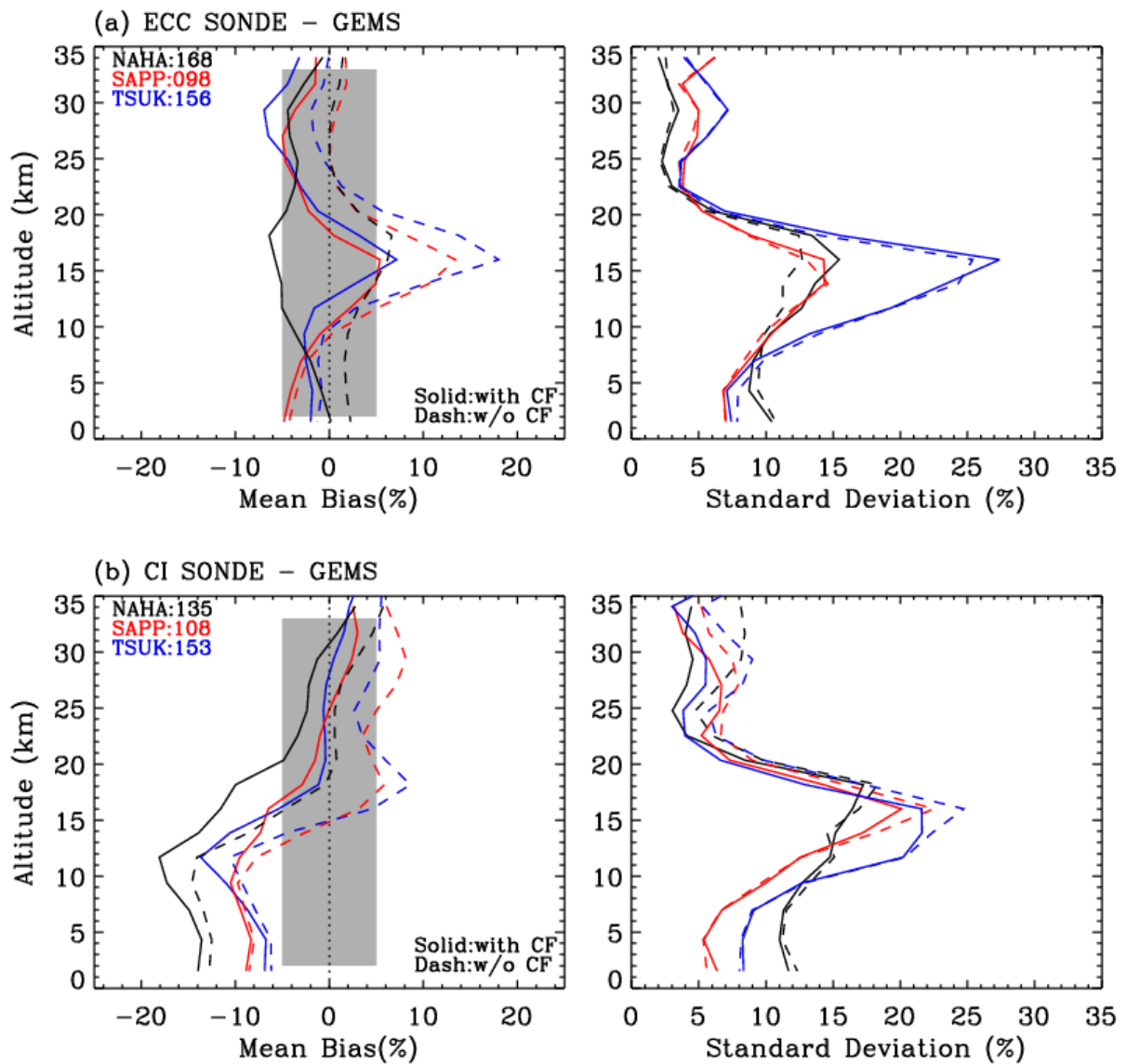


Figure 34. Effects of applying a correction factor (CF) to (a) ECC and (b) CI ozonesonde measurements, respectively, on comparisons with simulated GEMS ozone profile retrievals. Solid and dashed lines represent the comparisons with and without applying a CF, respectively, at each Japanese station. The number of data point is included in the legends.

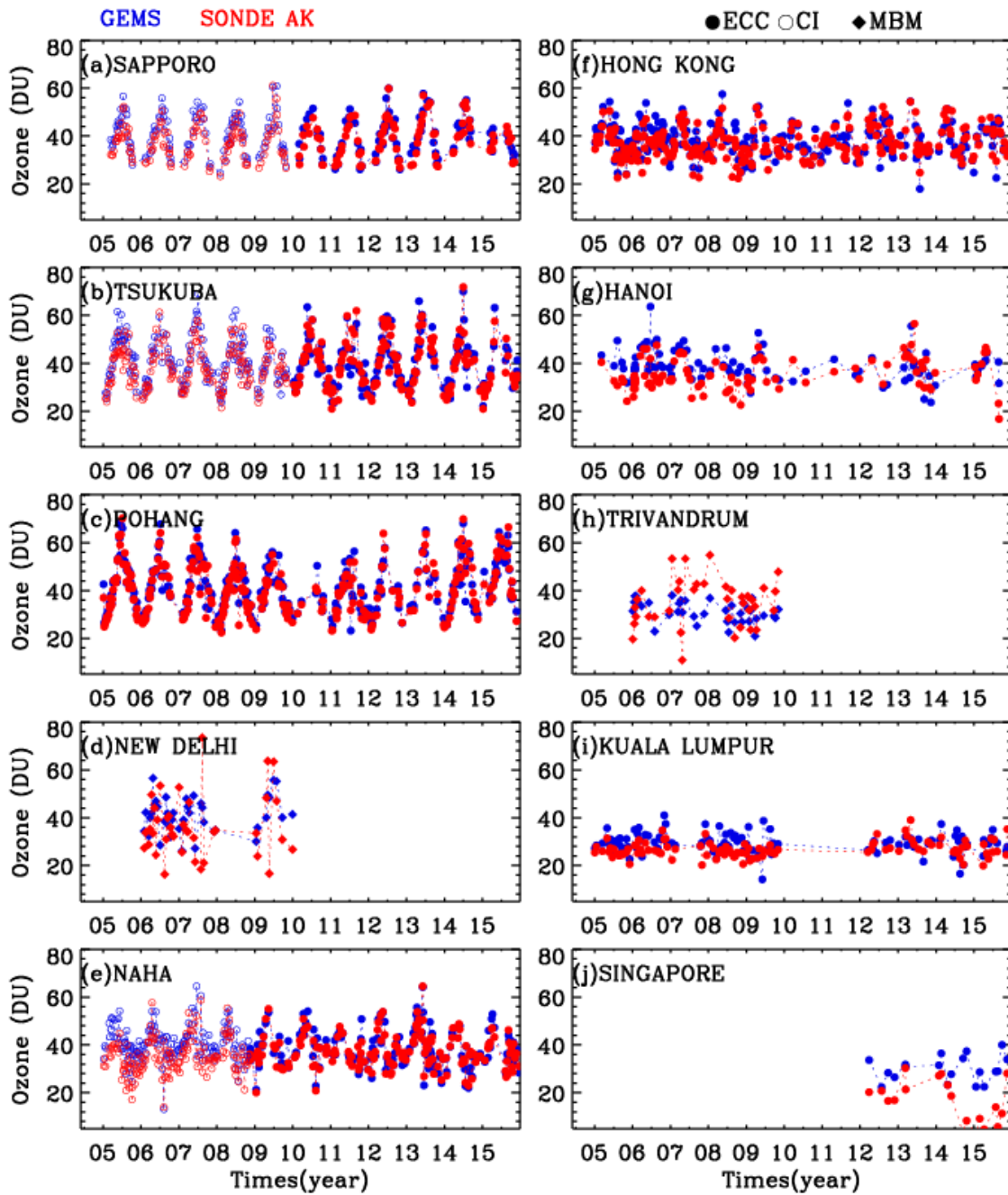


Figure 45. Time series of tropospheric ozone columns (DU) of GEMS simulated ozone profile retrievals (blue) and ozonesonde measurements convolved with GEMS averaging kernels (red) from 2005 to 2015 at 10 stations listed in Table 1.

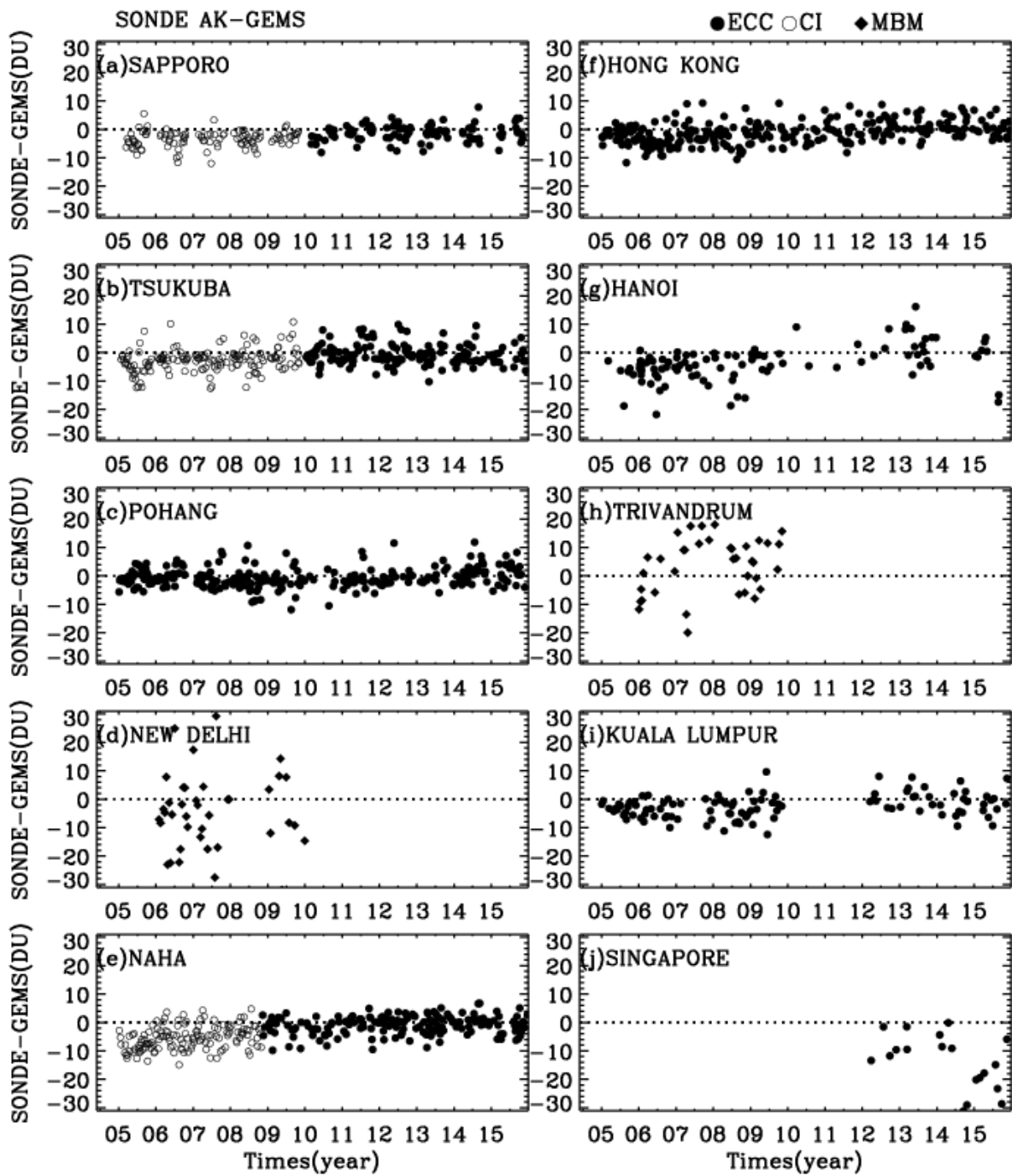


Figure 56. Same as Figure 45, but for absolute differences of tropospheric ozone columns (DU) between ozonesonde measurements and GEMS simulated retrievals.

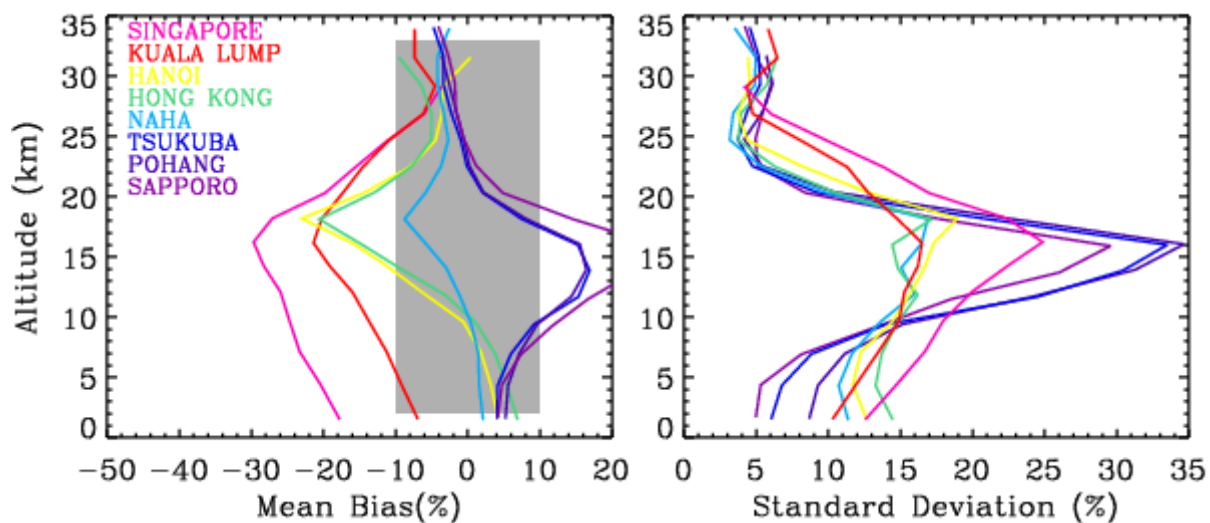


Figure 67. Mean biases and 1σ standard deviations of the differences between ozonesonde convolved with GEMS averaging kernels and GEMS simulated ozone retrievals as a function of GEMS layers, at individual ECC ozonesonde stations. The relative difference is defined as $\frac{2}{X} (\text{SONDE AK} - \text{GEMS}) \times 100\%$ (a priori).

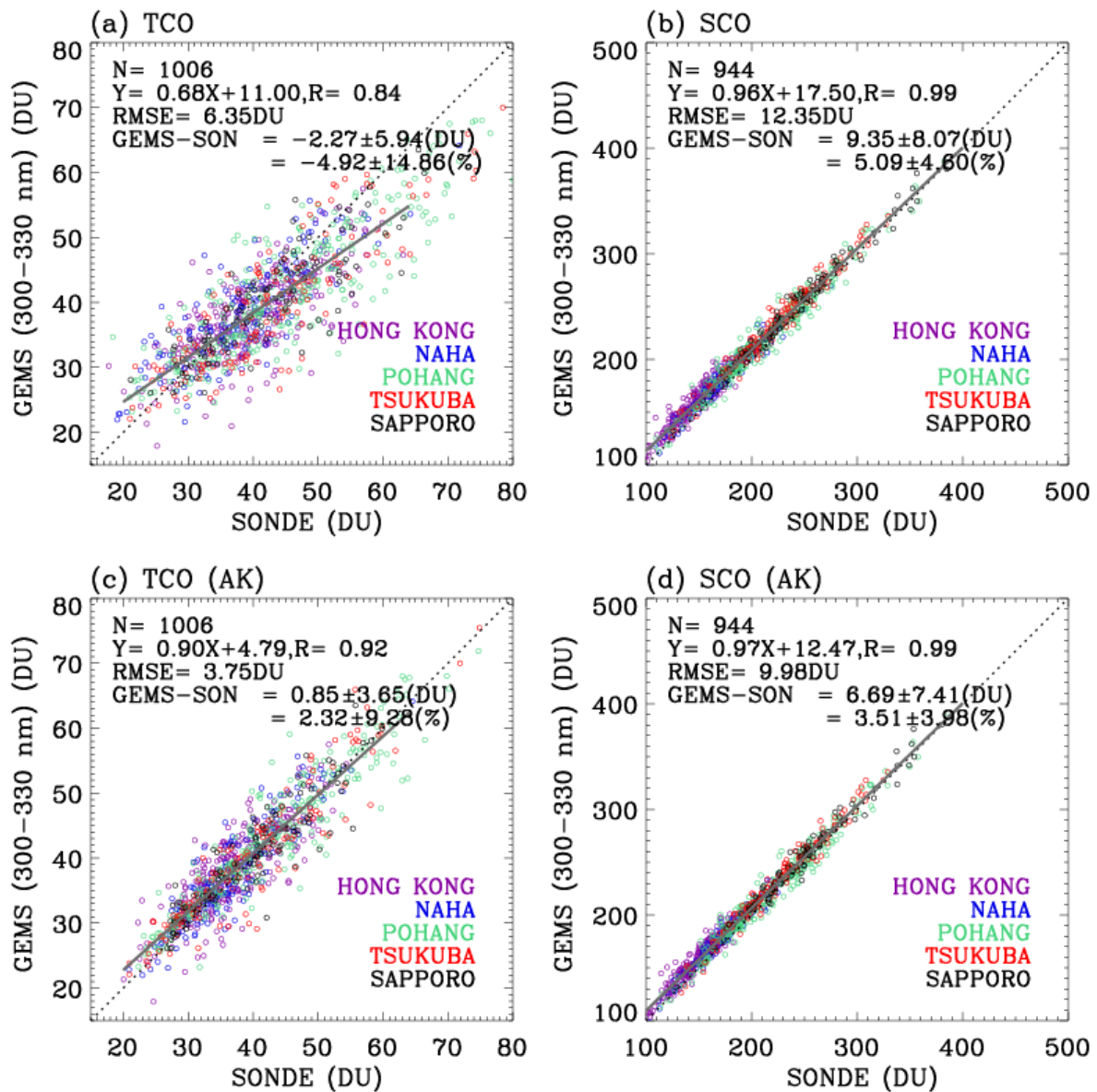


Figure 78. Upper: Scatter plots of GEMS vs. ozonesonde for tropospheric and stratospheric ozone columns, respectively. The lower panels is/are the same as the upper ones, except that ozonesonde measurements are convolved with GEMS averaging kernels. A linear fit between them is shown in red, with the 1:1 lines (dotted lines). The legends show the number of data points (N), the slope and intercept of a linear regression, and correlation coefficient (r), with mean biases and 1σ standard deviations for absolute (DU) and relative differences (%), respectively. Note that we use 5 stations identified as a good reference among 10 stations listed in Table 1 in this comparison.

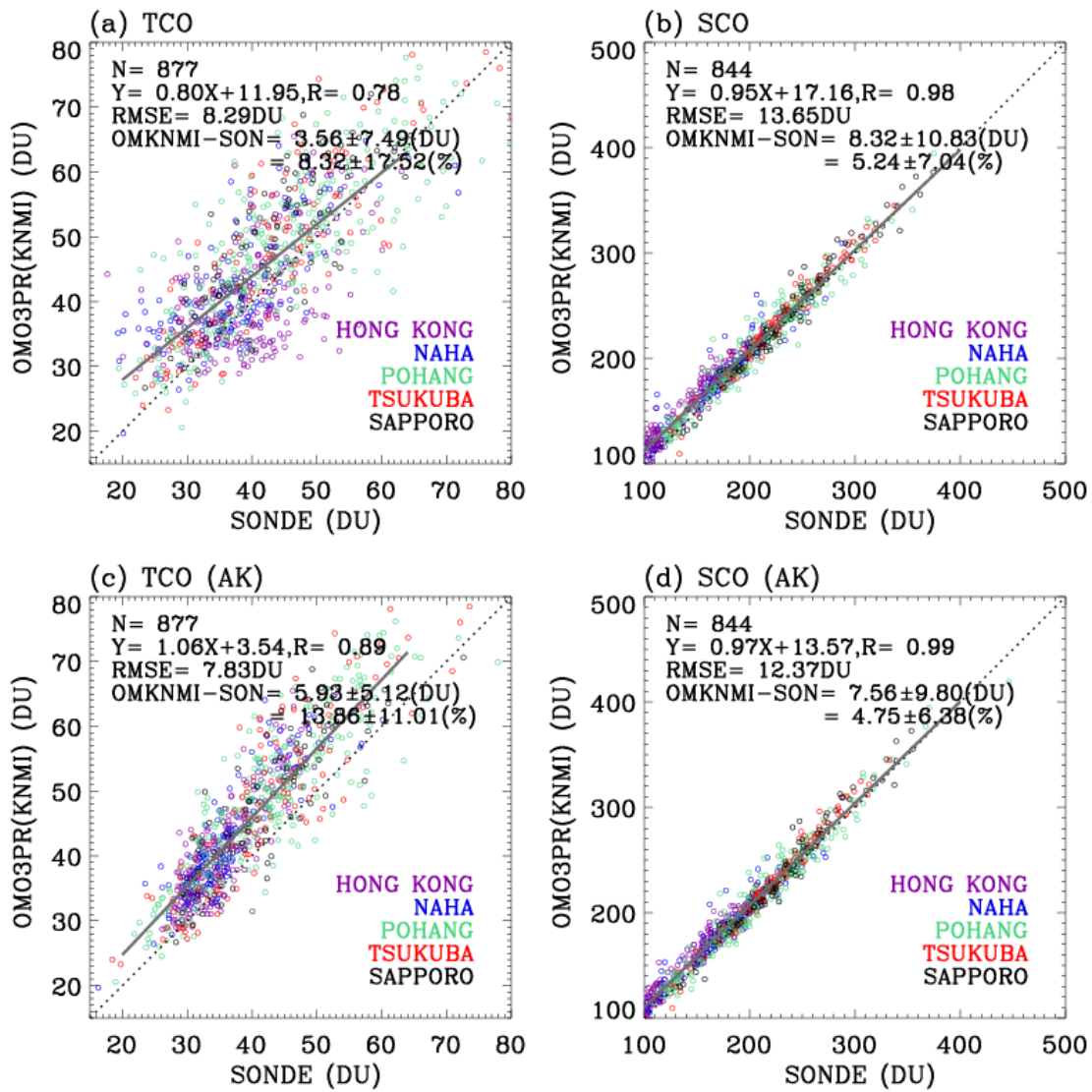


Figure 9. Same as Fig. 78, but for validating OMI standard ozone profiles (OMO3PR) produced by the KNMI optimal estimation OE-based algorithm.

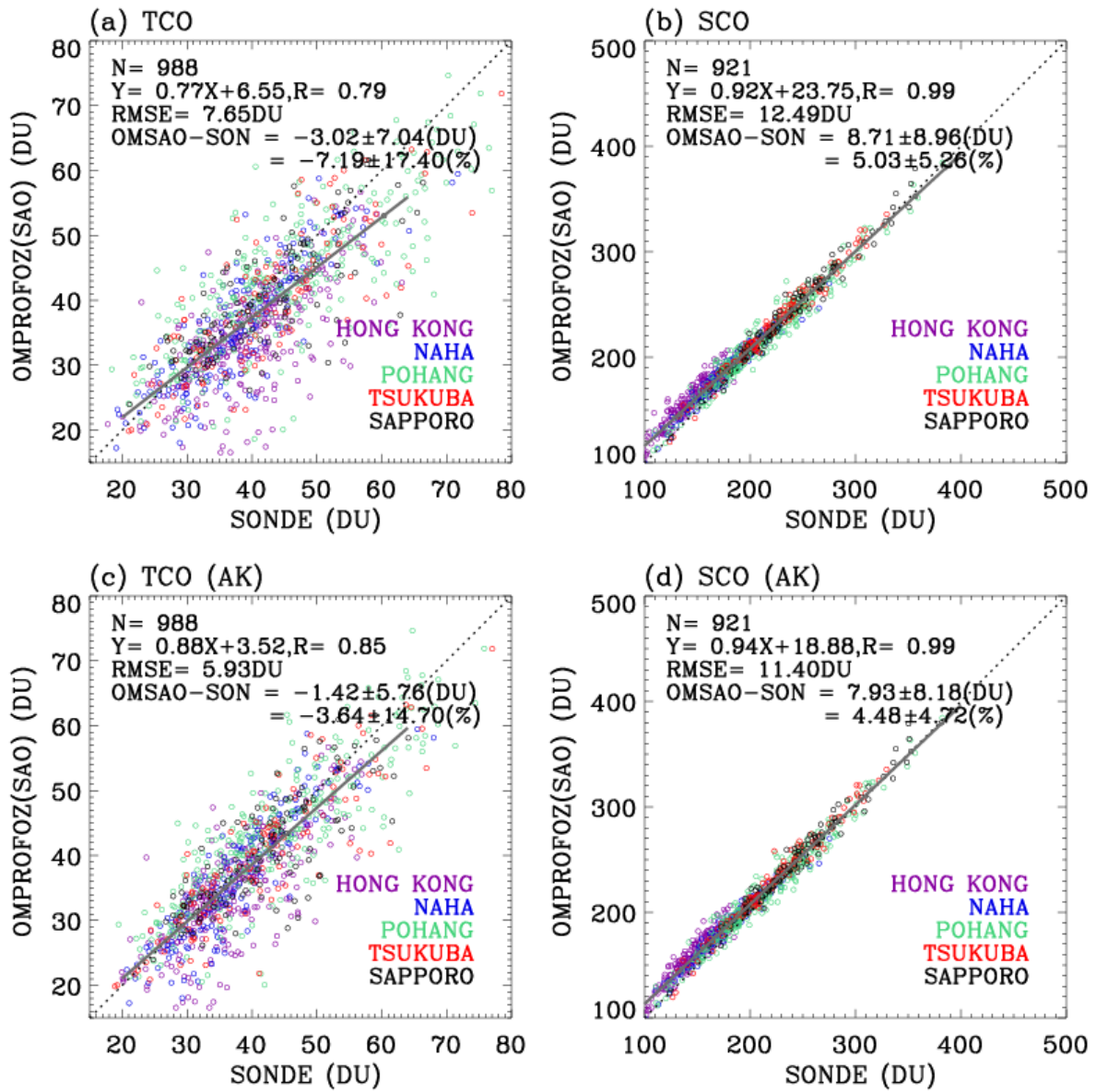


Figure 10. Same as Fig. 8, but for validating OMI research ozone profiles (OMPROFOZ) produced by the SAO optimal estimation (OE)-based algorithm.

Table1. List of ozonesonde stations.

Station ^a	Lon (°), Lat (°)	Altitude (m)	Observation Time ^b	Instrument Type ^c	ECC-SST ^d	Post Correction	
Singapore	103.9, 1.3	40	07:30-08:00 (9)	Jan 12 - Sep 15	ECC/EN-SCI Z	SST0.5	No correction
				Nov15 - Dec15	ECC/SPC 6A		
Kuala Lumpur	101.7, 2.7	20	9:30-15:00 (104)	Jan 13 - Dec14	ECC/SPC 6A	SST1.0	Transfer function
				Jan 15 - Dec15	ECC/EN-SCI Z	SST0.5	
Trivandrum	77.0, 8.5	60	14:00-14:30 (34)	Jan 06 - Dec11	MBM		Correction factor
Hanoi	105.8, 21.0	10	12:00-14:00 (42)	Jan 05 - Apr 06	ECC/EN-SCI 1Z	SST2.0	Transfer function
				Apr06 - Dec 07	ECC/EN-SCI 2Z	SST2.0	
				Jan 08 - May 09	ECC/EN-SCI 2Z	SST1.0	
				Jun 09 - Dec 09	ECC/SPC 6A	SST1.0	
				Feb 10 - Dec 11	ECC/EN-SCI Z	SST1.0	
				Feb 12 - Dec 13	ECC/EN-SCI Z	SST2.0	
				Jan 15 - Dec 15	ECC/EN-SCI Z	SST0.5	
Hong Kong	114.1, 22.3	70	13:00-14:30 (11)	Jan 05 - Dec 15	ECC/SPC 6A	SST1.0	No correction
Naha	127.7, 26.2	30	14:30-15:00 (06)	Jan 05 - Oct 08	CI/ KC-96	SST0.5	Correction factor
				Nov 09 - Dec 15	ECC/EN-SCI 1Z		
New Delhi	77.1, 28.3	270	11:00-14:30 (69)	Feb 06 - Dec11	MBM		Correction factor
Pohang	129.2, 36.0	40	13:30-15:30 (24)	Jan 05 - Dec 15	ECC/SPC 6A	SST1.0	No correction
Tsukuba	140.1, 36.1	330	14:30-15:00 (08)	Jan 05 - Nov 09	CI/ KC-96	SST0.5	Correction factor
				Dec 09 - Dec 15	ECC/EN-SCI 1Z		
Sapporo	141.3, 43.1	30	14:30-15:00 (06)	Jan 05 - Nov 09	CI/ KC-96	SST0.5	Correction factor
				Dec 09 - Dec 15	ECC/EN-SCI 1Z		

^a Data are downloaded from [the WOUDC \(http://woudc.org\)](http://woudc.org) data archive, except for Kuala Lumpur and Hanoi, which are from [the SHADOZ](#)

(<https://tropo.gsfc.nasa.gov/shadoz/>) network, and Pohang, which are from the Korea Meteorological Administration (KMA).

^b The range of the observation time (LT) with 1 σ standard deviations of them (min) in ~~the~~ parentheses.

^c Ozonesonde sensor type (ECC: Electrochemical Condensation Cell, CI: Carbon iodine cell Japanese sonde, MBM: Modified Brewer-Mast Indian sonde). ECC sensors manufactured by either ECC sensor manufactures; Science Pump Corporation (Model type: SPC-6A) and Environmental Science cooperation (Model type EN-SCI-Z/1Z/2Z).

Table 2. Comparison ~~Statistics~~ ~~statistics~~ (Mean ~~mean~~ Bias ~~bias~~ in DU, 1σ ~~Standard~~ ~~standard~~ Deviation ~~deviation~~ in DU, and R , ~~Correlation~~ ~~correlation~~ Coefficient ~~coefficient~~) between GEMS simulated ~~Tropospheric~~ ~~tropospheric~~ ~~o~~zone ~~c~~Column and ~~o~~zone ~~s~~onde ~~m~~Measurements convolved with GEMS averaging kernels.

Station	Collocation Time difference	Type	Data Period (Year)	SONDE AK – GEMS		
				#	Mean Bias + 1σ	R
Singapore	6:44	ECC	12-15	20	-13.67 ± 9.61	0.17
Kuala Lumpur	2:29	ECC	05-15	106	-2.54 ± 4.13	0.44
Trivandrum	1:46	MB-M	06-11	37	3.55 ± 9.75	0.24
Hanoi	0:32	ECC	05-15	100	-3.82 ± 6.03	0.52
Hong Kong	0:27	ECC	05-15	259	-1.19 ± 3.91	0.82
Naha	0:47	CI	05-08	135	-5.48 ± 4.07	0.85
		ECC	08-15	166	-0.94 ± 3.22	0.91
New Delhi	1:46	MB-M	06-11	39	-4.57 ± 13.36	0.24
Pohang	0:54	ECC	05-15	281	-0.75 ± 3.13	0.95
Tsukuba	1:56	CI	05-09	151	-2.98 ± 3.76	0.91
		ECC	09-15	154	-0.65 ± 3.53	0.94
Sapporo	2:18	CI	05-09	107	-3.43 ± 2.56	0.94
		ECC	09-15	95	-1.37 ± 2.79	0.93